

12-2015

## An Approach to Automotive Electrification and Testing

Christopher Rowe

Follow this and additional works at: <https://commons.erau.edu/edt>



Part of the [Electrical and Computer Engineering Commons](#)

---

### Scholarly Commons Citation

Rowe, Christopher, "An Approach to Automotive Electrification and Testing" (2015). *Dissertations and Theses*. 239.

<https://commons.erau.edu/edt/239>

This Thesis - Open Access is brought to you for free and open access by Scholarly Commons. It has been accepted for inclusion in Dissertations and Theses by an authorized administrator of Scholarly Commons. For more information, please contact [commons@erau.edu](mailto:commons@erau.edu).

AN APPROACH TO AUTOMOTIVE ELECTRIFICATION AND TESTING

By

Christopher Rowe

A Thesis Submitted to the College of Engineering Department of Electrical Engineering  
in Partial Fulfillment of the Requirements for the Degree of Master of Science in  
Electrical Engineering

Embry-Riddle Aeronautical University

Daytona Beach, Florida

December 2015

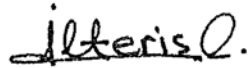
AN APPROACH TO AUTOMOTIVE ELECTRIFICATION AND TESTING

By

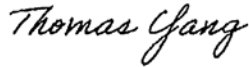
Christopher Rowe

This thesis was prepared under the direction of the candidate's Thesis Committee Chair, Dr. Ilteris Demirkiran, Department of Electrical and Computer Engineering, and has been approved by the thesis committee. It was submitted to the Department of Electrical and Computer Engineering and was accepted in partial fulfillment of the requirements for the degree of Master of Electrical and Computer Engineering.

Thesis Review Committee:



Ilteris Demirkiran, Ph.D.  
Committee Chair



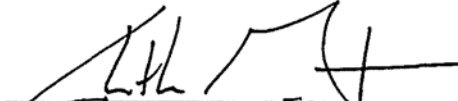
Thomas Yang, Ph.D.  
Committee Member



Patrick N. Currier, Ph.D.  
Committee Member



Maj Mirmirani, Ph.D.  
Dean, College of Engineering



Christopher Grant, Ph.D.  
Associate Vice President of Academics



Jianhua Liu, Ph.D.  
Master's Program Coordinator,  
Electrical and Computer Engineering

Date



# **1. Acknowledgements**

This thesis would not have been possible without the guidance and inspiration received from my thesis advisor, Dr. Ilteris Demirkiran, Dr. Thomas Yang, and also my EcoCAR advisor, Dr. Patrick Currier.

I would like to acknowledge my teammates on the Embry-Riddle EcoCAR 2-3 team that have spent countless hours working to build the 2013 Malibu

I would also like to thank the EcoCAR 2-3 competition, General Motors, and Argonne National Laboratory for providing the basis and inspiration for this research.

## 2. Abstract

Researcher: Christopher Rowe  
Title: An Approach to Automotive Electrification and testing  
Institution: Embry-Riddle Aeronautical University  
Degree: Master of Science in Electrical and Computer Engineering  
Year: 2015

In order to compete in the EcoCAR 2 competition, Embry-Riddle Aeronautical University has redesigned the Powertrain of a 2013 Chevrolet Malibu into a plug-in hybrid electric vehicle. This endeavor was made possible by the EcoCAR 2 competition sponsored by the Department of Energy, General Motors, and Argonne National Laboratory. The Powertrain was changed from a conventional internal combustion engine with start/stop capability, to a fully electric Powertrain, with a diesel generator, and plug in charging capability. This paper will cover the electrical work performed on the vehicle during the summer prior to year three of the competition, EcoCAR 2 year three, and preliminary work for EcoCAR 3 year one competition. The main focus of this paper will be on the electrical system integration and vehicle testing. Some of the systems include for EcoCAR 2 are the Selective Catalytic Reduction system, high voltage cabling optimization, CAN bus network, and charging system. For EcoCAR 3, the design and build of a high voltage distribution box, for bench testing, will be discussed. Simulations of the high voltage bus are also explored to gain insight into the voltage ripple and resonant frequency of the high voltage system in the vehicle.

### 3. Table of Contents

1.	Acknowledgements.....	iv
2.	Abstract.....	v
3.	Table of Contents.....	vi
4.	Table of Figures.....	viii
5.	Introduction.....	12
5.1	EcoCAR 2: Embry-Riddle Vehicle Architecture [2].....	13
5.1.1	Battery Pack.....	14
5.1.2	Powertrain Components.....	15
5.1.3	Power Generation Components.....	15
5.1.4	Plugin Charging Components.....	15
5.1.5	Regenerative braking.....	16
5.1.6	Diesel generator Power Plant.....	17
5.2	List of Acronyms.....	18
5.3	Thesis Statement.....	20
6.	Literature Review.....	21
7.	Methodology.....	26
7.1	Vehicle Wiring.....	26
7.1.1	Soldering Vs. Crimping and Wire Preparation.....	26
7.1.2	Wire Sizing.....	34
7.1.3	Fusing.....	36
7.2	SCR.....	40
7.3	Can Bus.....	43
7.4	HV Charging.....	44
7.5	GM vs. ERAU Drive Testing Procedure.....	48
7.6	HV Distribution Box.....	50
7.6.1	Demo Box Constraints.....	50
7.6.2	Demo Box Basic Design.....	51
7.6.3	Block Diagram.....	52
7.6.4	Schematic.....	53
7.6.5	HV Fusing.....	54
7.6.6	HV Test Connector Fusing.....	55
7.6.7	Torque Specifications.....	55
7.7	HV Simulation.....	56

8.	Results.....	62
8.1	Vehicle Wiring .....	62
8.1.1	Low Voltage .....	62
8.1.2	High Voltage .....	66
8.2	SCR .....	72
8.3	Can Bus .....	74
8.4	HV charging system design.....	76
8.5	Vehicle Testing .....	82
8.5.1	GM vs. ERAU Drive Test Results .....	82
8.5.2	Zero to Sixty.....	84
8.5.3	Regenerative Braking.....	85
8.5.4	Side Skirts Aero Test.....	87
8.6	HV Distribution Box Design.....	89
8.7	HV Simulation.....	94
9.	Conclusion .....	99
10.	Future work.....	100
11.	Bibliography .....	102



## 4. Table of Figures

Figure 1: Series PHEV General Architecture .....	12
Figure 2: ERAU Series Architecture .....	13
Figure 3: ESS Battery Pack.....	14
Figure 4: BRUSA HV Charger .....	16
Figure 5: Diesel Generator in Engine Bay .....	17
Figure 6: Frequencies Identified .....	24
Figure 7: frequency Range to Avoid.....	24
Figure 8: Voltage Ripple Experiment Results .....	25
Figure 9: Pre-Tinned Conductors.....	27
Figure 10: Soldered Conductors .....	27
Figure 11: Heat Shirked Connection.....	27
Figure 12: Pre-Tinned Conductors.....	28
Figure 13: Lashing of Pre-Tinned Conductors .....	28
Figure 14: Soldered Connection .....	28
Figure 15: Heat Shirked Connection.....	28
Figure 16: Initial Wrap for Western Union.....	29
Figure 17: Completed Wrap for Western Union.....	29
Figure 18: Soldered Western Union .....	29
Figure 19: Typical Crimping Tools .....	30
Figure 20: Butt Splice Prior to Wire Insertion.....	31
Figure 21: Butt Splice Prior to Crimp.....	31
Figure 22: Properly Crimped Butt Splice .....	31
Figure 23: Butt Splice with Heat Shrink.....	31
Figure 24: Wire with Weather Seal .....	32
Figure 25: Wire with no Weather Seal .....	32
Figure 26: Typical Crimps Terminal Pins .....	32
Figure 27: Sealed Terminal.....	32
Figure 28: Unsealed Terminal .....	33
Figure 29: Crimped Terminals.....	33
Figure 30: Wire Strippers.....	33
Figure 31: Proper Wire .....	34
Figure 32: Extra Insulation .....	34
Figure 33: Nicked Insulation .....	34
Figure 34: Over twist .....	34
Figure 35: Bent Conductors.....	34
Figure 36: Nicked / Cut Conductors .....	34
Figure 37: Crushed Conductor.....	34
Figure 38: Common Automotive Fuses.....	38
Figure 39: Fuse Time-Current Characteristic Curves.....	40
Figure 40: SCR Schematic.....	42
Figure 41: CAN Bus Signals.....	43
Figure 42: Basic CAN Bus Diagram .....	44
Figure 43: J1772 Schematic [10] .....	46
Figure 44: Charging Schematic .....	47
Figure 45: Aerodynamic Modifications.....	50

Figure 46: 2D CAD Drawing.....	51
Figure 47: HV Demo Box Block Diagram .....	52
Figure 48: HV Fuse Curve.....	55
Figure 49: HV Simulation Simulink Model.....	57
Figure 50: Model Measurements .....	57
Figure 51: ESS Battery Subsystem.....	59
Figure 52: HVAC Subsystem .....	59
Figure 53: BRUSA Subsystem .....	60
Figure 54: Inverter Subsystem.....	61
Figure 55: DC/DC Subsystem .....	61
Figure 56: Bad Crimp w/ Insulation Crushed.....	63
Figure 57: Bent Crimp .....	63
Figure 58: Lack of Conductor in Crimp .....	63
Figure 59: Inverter Configuration 0 Wiring.....	65
Figure 60: Inverter Configuration 1 Wiring.....	65
Figure 61: New 12V Distribution .....	65
Figure 62: Inside 12V Distribution Box .....	66
Figure 63: HV Block Diagram.....	67
Figure 64: HV Before Length Reduction.....	68
Figure 65: HV After Length Reduction .....	68
Figure 66: Inside Front DDE .....	68
Figure 67: HV Cable Sleeving Test.....	69
Figure 68: HV Cable, Med. Force, 10 reps.....	69
Figure 69: Sleeving, Med. Force, 10 reps.....	70
Figure 70: Sleeving, Heavy Force, Until Failure.....	70
Figure 71: Traction Motor with Gland Plate Removed .....	71
Figure 72: NH <sub>3</sub> Sensor .....	72
Figure 73: SCR Tank and Body to SCR Harness Connector .....	72
Figure 74: NH <sub>3</sub> Injector .....	73
Figure 75: SCR Power Distribution Box .....	73
Figure 76: Old ERAU CAN.....	75
Figure 77: New ERAU CAN.....	75
Figure 78: Vehicle signal Diagram.....	76
Figure 79: Charging Simulation.....	77
Figure 80: Vehicle Proximity and Control Pilot Controller.....	78
Figure 81: Control Pilot Normal Operation .....	80
Figure 82: Control Pilot Fault.....	81
Figure 83: Level 1 120V Charge .....	81
Figure 84: Level 2 220V Charge .....	81
Figure 85: GM Test Data .....	83
Figure 86: ERAU Test Data.....	83
Figure 87: Vehicle 0 to 60 mph data.....	85
Figure 88: Regenerative Braking Data .....	86
Figure 89: Aero Test No Side Skirts.....	88
Figure 90: Aero Test with Side Skirts.....	88
Figure 91: HV Cable step 1 .....	90

Figure 92: HV Cable step 2 .....	90
Figure 93: HV Cable step 3 .....	90
Figure 94: HV Cable step 4 .....	90
Figure 95: HV Cable step 5 .....	90
Figure 96: HV Cable step 6 .....	90
Figure 97: HV Cable step 7 .....	90
Figure 98: Cable Ends.....	90
Figure 99: HV Hardware .....	91
Figure 100: Plexiglas .....	91
Figure 101: Separators .....	91
Figure 102: Copper Shielding.....	91
Figure 103: GND Plate .....	91
Figure 104: Enclosure .....	91
Figure 105: Gland Apart .....	91
Figure 106: Gland Together.....	91
Figure 107: Shielding in Box.....	92
Figure 108: Plate with Hardware .....	92
Figure 109: Glands Installed.....	92
Figure 110: Cables Installed .....	92
Figure 111: Test Conn. & HVIL.....	92
Figure 112: Box Insulated.....	92
Figure 113: Box Labels 1.....	92
Figure 114: Box Labels 2.....	92
Figure 115: Box Labels 3.....	92
Figure 116: HV test Connector and HVIL Micro Switch.....	93
Figure 117: HV Box Complete .....	93
Figure 118: Power Spectral Density 12 kHz.....	95
Figure 119: DC Bus Voltage 12 kHz.....	96
Figure 120: Spectrum Analyzer 12 kHz .....	96
Figure 121: Power Spectral Density 911 Hz.....	97
Figure 122: DC Bus Voltage 911 Hz.....	98
Figure 123: spectrum Analyzer for 911 Hz .....	98

Table of Tables	
Table 1: AWG Wire Table.....	36
Table 2: ATM Cooper Bussmann Automotive Fuses.....	39
Table 3: BRUSA Charging Characteristics .....	45
Table 4: HV demo box constraints .....	50
Table 5: Bolt Torque Specs.....	56
Table 6: ESS Battery Characteristics .....	58
Table 7: Control Pilot and Proximity States [10].....	77
Table 8: Vehicle Test Data .....	82
Table 9: Simulation Calculated Characteristics .....	94

## 5. Introduction

EcoCAR 2 is a three year competition sponsored by the Department of Energy, General Motors, and Argonne National Laboratory. The competition encompasses fifteen Universities across North America [1]. A 2013 Chevrolet Malibu is donated to each team where it is converted to an electric hybrid vehicle. EcoCAR 2 challenges students to reduce the Chevrolet Malibu's emissions, increase fuel economy, and maintain consumer acceptability [1]. The mission of EcoCAR 2 is to educate the next generation of automotive engineers through an unparalleled hands-on, real-world engineering experience. [2]

In this competition, Embry-Riddle Aeronautical University chose to design and build a plug-in hybrid electrical vehicle (PHEV) using a series architecture. Figure 1 shows the general series architecture of an electric PHEV. The traction motor, generator, and internal combustion engine are in the engine bay of the vehicle. The ESS is in the trunk. The black arrows represent the flow of mechanical energy, and the yellow arrows represent electrical energy. [2]

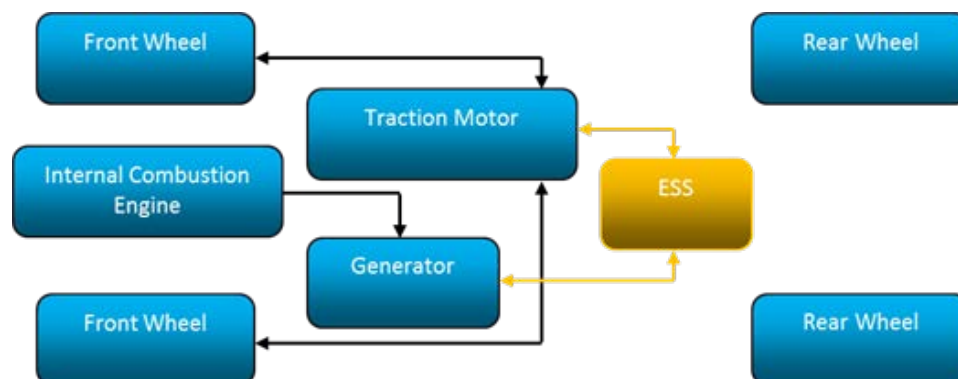


Figure 1: Series PHEV General Architecture

Series plug-in hybrid vehicles consist of one or more electric motors driving the wheels, and these motors are powered by a battery. An engine-generator is decoupled from the wheels at all times and provides supplemental electrical power to drive the vehicle when needed while charging the battery pack at the same time.

### 5.1 EcoCAR 2: Embry-Riddle Vehicle Architecture [2]

The placement of major components is represented in Figure 2. The front of the vehicle is located where the traction motor is located.

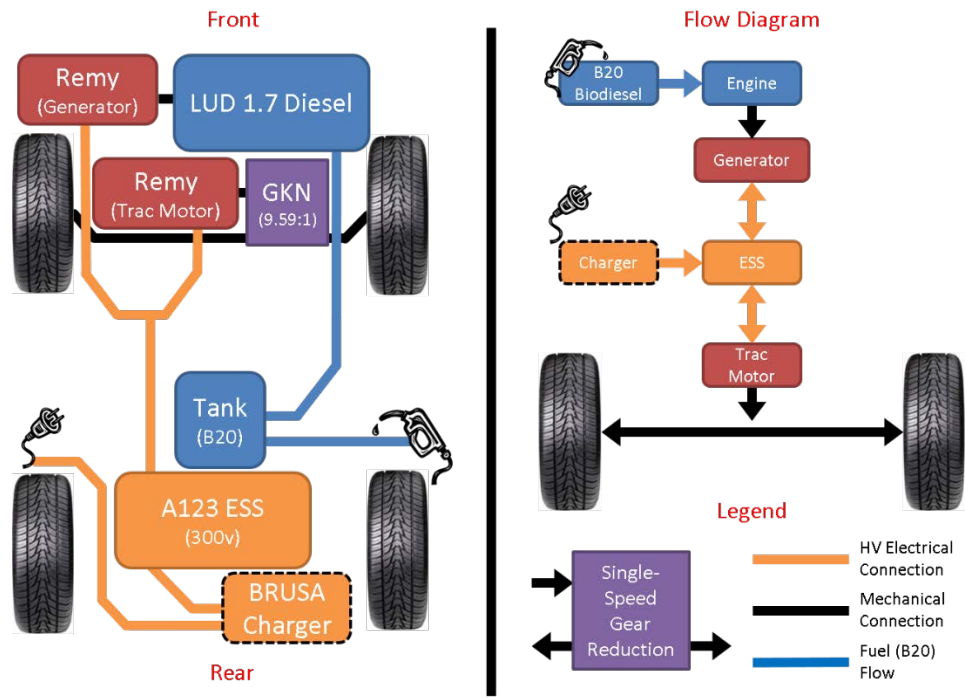


Figure 2: ERAU Series Architecture

### 5.1.1 Battery Pack

The Energy Storage Unit (ESS), seen in Figure 3, is composed of six 15S3P LiFePO<sub>4</sub> battery modules from A123. All the modules are in series to get a nominal pack voltage of 292V.

In order to monitor the modules, a battery management system (BMS) is used within the ESS. The BMS collects data from each module to track each cell's voltage level and temperature. The BMS also monitors the ESS voltage and current levels. The BMS is necessary in order to ensure the modules are being charged and discharged correctly to mitigate the chance of causing damage to the modules within the ESS. If a problem is identified, the BMS will open the contactors connected to the battery modules in order to disconnect the ESS from the rest of the vehicle's high voltage (HV) systems.



Figure 3: ESS Battery Pack

### 5.1.2 Powertrain Components

The main powertrain components consist of an AM Racing Remy HVH 250-090P Traction Motor which is coupled to a GKN E-Transmission. As a Series Plug-In Hybrid, the tractive force supplied to the wheels of the vehicle solely comes from the electric traction motor.

### 5.1.3 Power Generation Components

The full electric range of the vehicle is 30 to 40 miles, depending on traffic and driver habits. To improve consumer acceptability a 1.7 liter GM Diesel Engine coupled to an AM Racing Remy HVH 250-090S Generator was installed in the vehicle. This genset acts as a range extender by supplying electrical power to the traction motor and ESS. This allows the vehicle to keep driving after the ESS has been depleted. The diesel engine does not provide any torque to the tires of the vehicle.

### 5.1.4 Plugin Charging Components

The vehicle is equipped with a BRUSA NLG5 Battery Charger as seen in Figure 4. This enables the vehicle to utilize the AC mains of 120 VAC or 220 VAC. If 120 VAC is used the BRUSA will operate in a reduced power mode limited to a 1 kW output; however, by using 220 VAC The BRUSA charger will be able operate at its peak output of 3.3 kW.





Figure 4: BRUSA HV Charger

The BRUSA inverts the AC power into DC to charge the battery. In order to charge the  $\text{LiFePO}_4$  cells in the pack properly, the BRUSA communicates with the battery management system, located in the ESS, with CAN bus messages to control the charging process.

### 5.1.5 Regenerative braking

By using an AC Interior Permanent Magnet (IPM) electric motor (AMR-250P), regenerative braking can be used for two purposes. The primary purpose is to generate power back to the battery pack while slowing the vehicle. By recovering this power while braking, the vehicle is able to extend the time and mileage while the vehicle is operating in EV mode only. This is important since the longer the vehicle stays in the charge deplete mode (CD) the longer the diesel engine will stay off. This will reduce the overall vehicle emissions greatly.

The second purpose of regenerative braking is to enhance the EV driving experience. By using a zero floating point controls strategy, it is possible to drive the vehicle using mostly the acceleration pedal. It is only necessary to use the brake pedal when the vehicle is below ~10 MPH or greater braking is required, but for normal city or highway driving the regenerative braking provides enough braking power to comfortably drive the vehicle with only the acceleration pedal.

### 5.1.6 Diesel generator Power Plant

Once the ESS has been depleted to a depth of discharge (DOD) of 20% the vehicle will enter a charge sustain mode (CS). CS will enable the vehicle to continue driving while the ESS is in need of charging. In conventional EVs the vehicle must stop driving and plug-in to charge the ESS, and once the ESS has been re-charged the vehicle can continue driving. Under CS mode the vehicle will allow the ESS to deplete to 20% and then turn on a diesel electric generator, seen in Figure 5, to provide power to the ESS and traction motor.



Figure 5: Diesel Generator in Engine Bay

## 5.2 List of Acronyms

	AC	Alternating Current
	APM	Auxiliary Power Module
	AWG	American Wire Guage
	BCM	Body Control Module
	BMS	Battery Management System
	CAN	Controller Area Network
	CAT	CATalytic converter
	CD	Charge Depletion
	CP	Control Pilot
	CS	Charge Sustaining
	DC	Direct Current
	DDE	Distribution and Disconnect Enclosure
	DPF	Diesel Particulate Filter
	E&EC	Emissions and Energy Consumption
	EMS	Energy Management Strategy
	ERAU	Embry-Riddle Aeronautical University
	ESS	Energy Storage System (high voltage battery pack)
	EV	Electric Vehicle
	EVSE	Electric Vehicle Supply Equipment
	GM	General Motors
	GND	Ground
	HIL	Hardware In the Loop

	HV	High Voltage
	HVAC	High Voltage Air Conditioning
	HVIL	High Voltage Interlock Loop
	ICE	Internal Combustion Engine
	LV	Low Voltage
	MABX	Microautobox
	MPG	Miles Per Gallon
	MY	Model Year
	NOx	Nitrogen Oxide
	PHEV	Plug-in Hybrid Electric Vehicle
	PROX	Proximity
	PSD	Power Spectrum Density
	PWM	Pulse Width Modulated (Square wave)
	RPM	Revolutions Per Minute
	SAE	Society of Automotive Engineering
	SCR	Selective Catalytic Reduction
	SIL	Software In the Loop
	SOC	State of Charge
	VAC	Voltage Alternating Current
	YR	Year
	WOT	Wide Open Throttle

### 5.3 Thesis Statement

This paper investigates the strong hybridization of a conventional production vehicle. The creation of a series plug-in hybrid electric vehicle with extended range capabilities will be investigated pertaining to the vehicle electrical systems. The main focus will be on HV and LV system modifications performed on a 2013 Malibu. A secondary focus will be explored to estimate voltage ripple and resonant frequency by using on HV bus simulations.

## 6. Literature Review

The basis for this literature review is based around the high voltage simulation designed for this thesis. While researching papers for electric vehicle high voltage bus characterization, it became evident there has been little work performed on the high voltage bus, encompassing the entire bus and HV components, of electric vehicles. In dealing with resonant frequency, the main focus for research leans toward leveraging resonant frequency for charging electric vehicles [3]. One such paper titled “Current Ripple Reduction in 4kW LLC Resonant Converter Based Battery Charger for Electric Vehicles” describes a resonant controller employed to suppress the low-frequency current ripple in an LLC resonant converter for EV battery chargers [3]. A part of this paper has a study with a focus on the affect voltage ripple in the DC-link capacitor, or bulk capacitor, has within the charger. The point this paper makes is that a small change in voltage on the DC-link capacitor can result in a large change in ripple current; however, the voltage ripple in the DC-link capacitor is set to 12 V peak to peak and does not change [3]. The paper does not look at how the charger can induce the voltage ripple in the DC-link capacitor. This would be a more accurate representation of the cause of voltage ripple on the system. This paper also is focused on the charging side of the vehicle dealing with the switching characteristics of the vehicle charger. Although, the HV simulation of this thesis focuses on the inverter switching characteristics, both charging and inverter switching characteristic topologies are very similar.

To help aid in designing the HV simulation a book titled “Introduction to Hybrid Vehicle System Modeling and Control” was very useful. This book focuses on modeling,

control, simulation, and performance analysis of specific systems of electric vehicles. Vehicle architectures are also discussed with detail in component characterization, and a systematic approach to develop models, controls, and algorithms [4]. “The Electrical Engineering Handbook” aided in battery characterization and simple models of a battery. This book also went in depth into the workings of Inverter switching techniques along with different methods of powering electric motors with inverters [5]. This helped design the switching characteristics in the HV simulation described in this paper to more closely model the proper switching of an inverter.

“Co-Simulation and Harmonic Analysis of a Hybrid Vehicle Traction System” explores a modern hybrid vehicle design where a three phase traction motor, powered by an inverter, is connected to a high voltage battery. In order to determine the high frequency system behavior, the current and voltage harmonics of this system are simulated to estimate the effect from the switching in the inverter [6]. A frequency analysis was performed on the bus, from the battery to the inverter, by analyzing the DC bus current ripple. A frequency of 20 kHz was identified to have the largest power [6]. The model used to characterize the system has a heavy focus on the inverter itself; however, the model does not consider any other components commonly seen in electric vehicles. The inverter does have a major influence on the system; however, modern vehicles no longer simply have a battery and a traction inverter in the HV electrical system.

“Development and Future Issues of High Voltage Systems for FCV” details a vehicle designed by the Nissan Motor Co., Ltd. The vehicle delivered was the 2005 X-

TRAIL FCV, and was available to customers on April 2006 in Japan [7]. This paper details the vehicles architecture as well as the workings of a DC/DC converter used in the vehicle to boost the vehicle voltage from a fuel cell to power the traction inverter. By using a DC/DC converter to amplify bus voltage the voltage ripple on the bus is amplified. This is due to having both the DC/DC converter and traction inverter on the same bus while switching at the same time. This paper does not go into detail of what problems could arise from multiple high power switching devices operating at the same time [7]. This is a similar issue in the HV simulation designed for this thesis. There can be two inverters providing power to motors in the simulation designed.

“Design Considerations for High-Voltage DC Bus Architecture and Wire Mechanization for Hybrid and Electric Vehicle Applications” notes that modern hybrid electric vehicle no longer have simple HV DC bus designs. Current vehicles have multiple power converters units and energy storage systems on a single bus [8]. The author also correctly identifies the fact that each component should meet a set of common HV bus design requirements besides their own functional requirements. Because of this fact the author is looking at the system as a whole instead of single components. This paper describes HV DC bus architecture and component selection particularly for Extended-Range Electric Vehicle application [8]. Multiple architecture layouts are looked at in this paper; however, the main focus is on voltage ripple, resonance and voltage transients during various vehicle drive profiles. The author is able to identify a frequency range that should be avoided during vehicle operation seen in Figure 6 and Figure 7 [8].



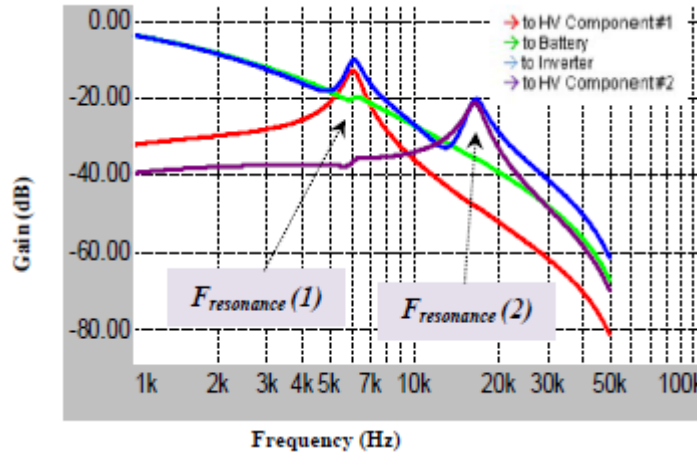


Figure 6: Frequencies Identified

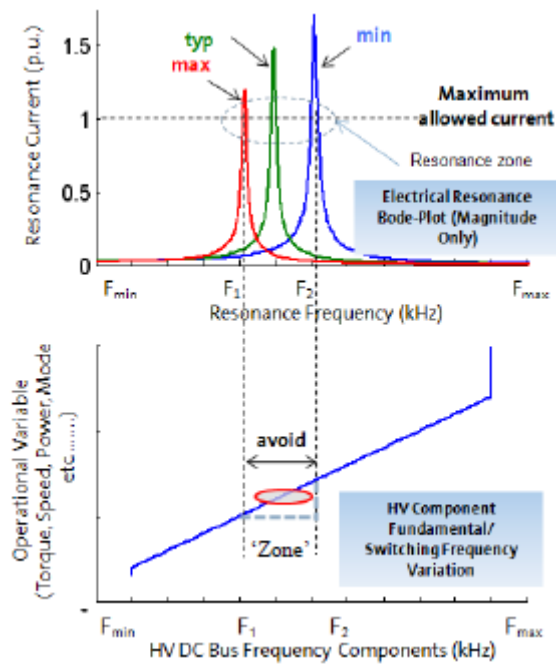


Figure 7: frequency Range to Avoid

The author identifies the traction inverter as being the biggest power converter in the HV bus system. Due to this, the author analyzes target vehicle drive conditions and identifies critical usage profiles for the inverters. These critical profiles represent worst case HV bus ripple generated by the inverter [8]. This is used as the basis for the voltage ripple study. The simulated data from this paper focuses more on voltage transients the

actual voltage ripple; however actual experimental data is gathered showing the actual voltage ripple and is compared to simulation data. The results of this experiment can be seen in Figure 8 [8].

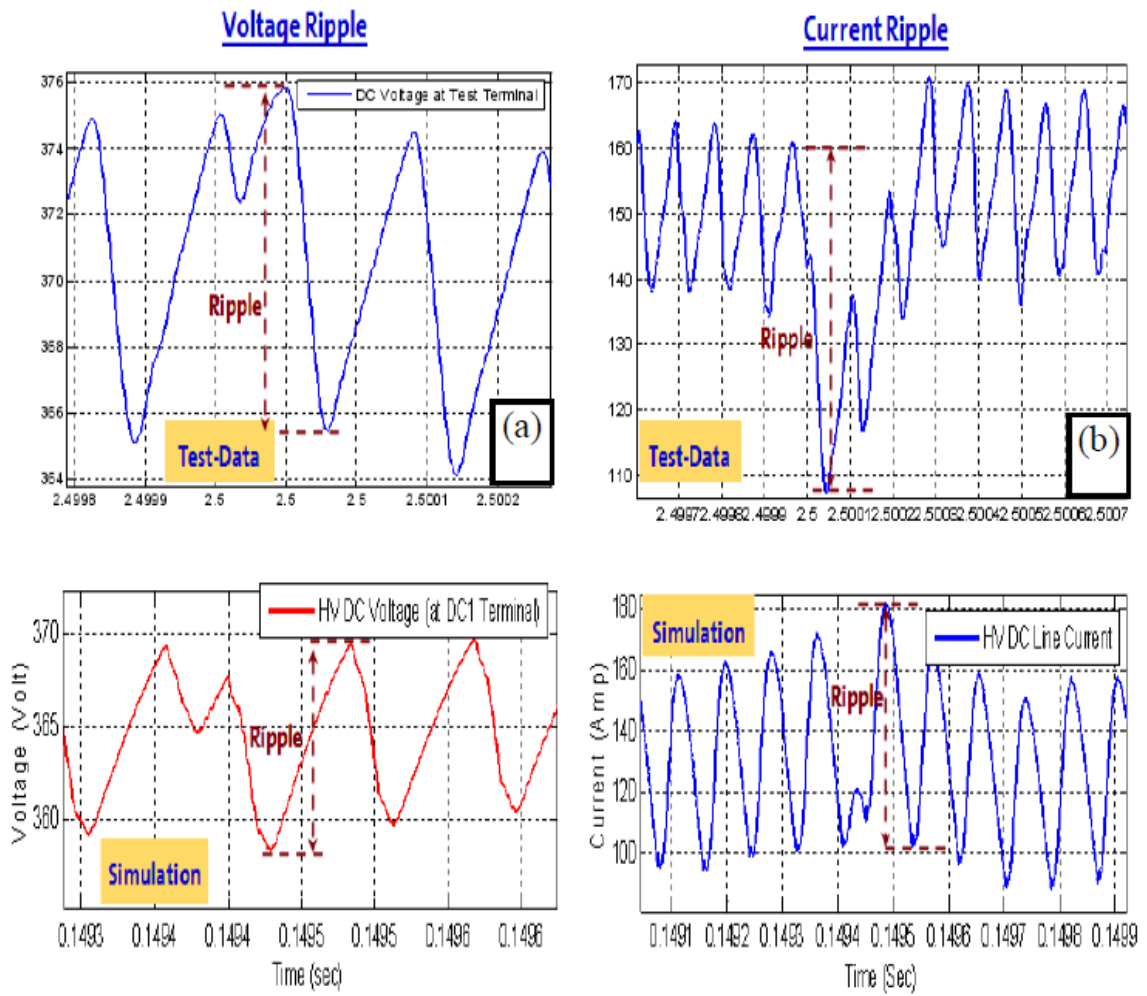


Figure 8: Voltage Ripple Experiment Results

## **7. Methodology**

### **7.1 Vehicle Wiring**

#### **7.1.1 Soldering Vs. Crimping and Wire Preparation**

There is an ongoing debate which has been going on for years dealing with circuits being soldered or crimped. Soldered wires are thought to be brittle and can break overtime; while, crimped wires are thought to not hold together well over time causing the wire to release from the crimp. The truth is both soldering and crimping are valid ways to connect circuits and terminate wires with terminals. For automotive specifically, the OEMs go the route of crimping almost exclusively. This is due to the vibrations in a vehicle, and the thought is crimps hold up better to the vibrations. NASA on the other hand uses soldering on the space shuttle, and it experiences heavy vibrations when launching into space. The important fact is that each method is performed correctly to prevent potential failures.

##### **7.1.1.1 Soldering**

There are several methods for soldering conductors together. The most common techniques are the lap splice, lash splice, and the western union. With each splice it is important to use just enough solder to form the connections. Too much solder can wick into the conductor and go under the insulation. This will cause the wire to become stiff and could break over time. If not enough solder is used the conductors can pull apart. In most

cases too much solder is usually used. The proper amount of solder will allow a solid connection between conductors; however, the individual strands of the conductors should still be able to be seen as in Figure 10.

A lap splice solders conductors together with each conductor straight and soldered length wise. The conductors should be pre-tinned before soldering the conductors together. This will aid in the transfer of heat during the soldering process. Heat shrink should be used to cover the connection when finished. A quarter inch of insulation should be removed for this splice. This process is seen in Figure 9, Figure 10, and Figure 11 [9].



Figure 9: Pre-Tinned Conductors

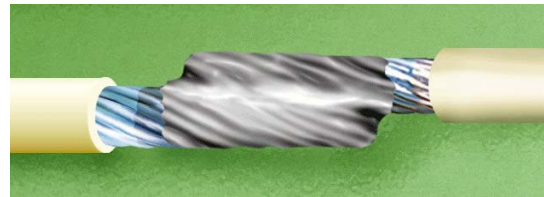


Figure 10: Soldered Conductors



Figure 11: Heat Shirked Connection

The lash splice is similar to the lap splice. It adds a single strand of wire to “lash” the pre-tinned conductors together. The extra strand is used to wrap around the conductors to aid in the soldering process by holding the wires together. This is especially beneficial

when a person is soldering by themselves, and cannot hold the wires and soldering iron at the same time. Heat shrink should be used to cover the connection when finished. A quarter inch of insulation should be removed for this splice and the single strand should be half an inch long. This process is seen in Figure 12 through Figure 15 [9].



Figure 12: Pre-Tinned Conductors

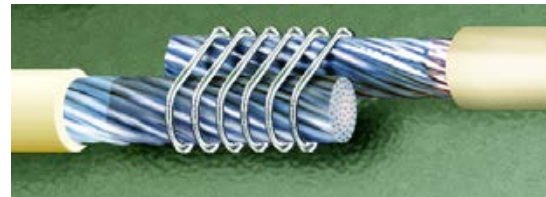


Figure 13: Lashing of Pre-Tinned Conductors



Figure 14: Soldered Connection



Figure 15: Heat Shirked Connection

The western union splice is the most common splice used. The wires can be pre-tinned prior to solder, but very little solder can be used to aid in wrapping the wires together. The conductors are wrapped together with at least three turns around each conductor. This makes sure the conductors will not come apart during the soldering process. Like the previous splices, just enough solder should be used to connect the conductors together. The conductor strands will still be visible through the solder. A half inch of insulation should be removed from each conductor for this splice. This process is seen in Figure 16 through Figure 18 [9].

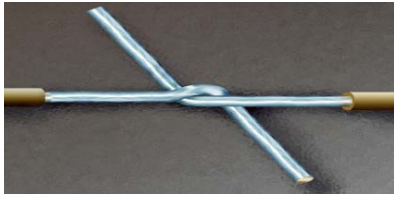


Figure 16: Initial Wrap for Western Union



Figure 17: Completed Wrap for Western Union



Figure 18: Soldered Western Union

### 7.1.1.2 Crimping

Crimping is another viable method for connecting circuits together. Crimping uses mechanical force to form connections. The amount of force applied to the crimp must be just right. Too much force and the conductors can be crushed, and too little force will likely result in the conductor falling out of the crimp. Special tooling is required for each different crimp to ensure the crimp will not fail prematurely. Figure 19 shows the tooling typically used for crimping. Each kind of crimp has a matching tool to perform the job. The better tools use a ratcheting feature which will not release the tool until the proper force has been applied to the crimp. Once the right amount of force is applied the ratcheting feature will allow the tool to release.



Figure 19: Typical Crimping Tools

Crimping is performed for two main reasons. The first is to connect separate conductors together, and the second reason is to crimp a terminal pin to the end of a wire for insertion into a connector. For vehicles, crimping is mostly done to connect terminal pins to the ends of wires. Just like soldering, the insulation of the wire must be stripped off the conductor before crimping, and the amount of insulation removed depends on the type of crimp being performed. The amount of insulation removed is usually a quarter of an inch.

Butt splices are used to crimp multiple conductors together. The number of conductors can be easily adjusted using this crimping method. Two wires are usually connected; however, multiple wires can be inserted into a single end of the butt splice. To do this, the total number of wires cross-sectional areas must add up to what the butt splice is rated for. If the added cross-sectional area is greater than what the butt splice is rated for then the wires will either not fit, or the conductors will be crushed when crimped. If the added cross-sectional area is less than what the butt splice is rated for then the wires will fall out of the butt splice. To properly prepare a wire for a butt splice, the wire should be inserted into the butt splice for an initial measurement for trimming the insulation. The insulation should not enter the butt splice, and about a millimeter of the conductor should

be seen between the insulation and butt splice. There is also a hole in the middle of the butt splice. This is used to ensure the conductor is inserted fully into the butt splice. The butt splice process is seen in Figure 20 through Figure 23 [9].

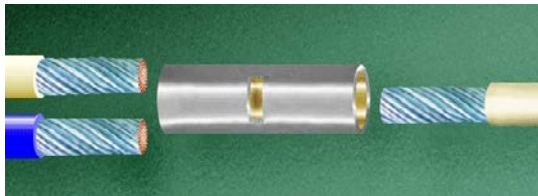


Figure 20: Butt Splice Prior to Wire Insertion



Figure 21: Butt Splice Prior to Crimp

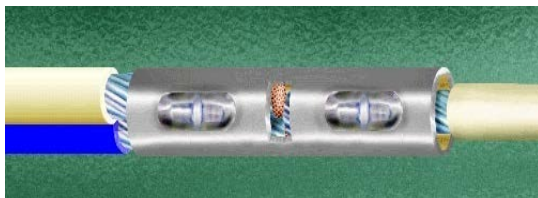


Figure 22: Properly Crimped Butt Splice

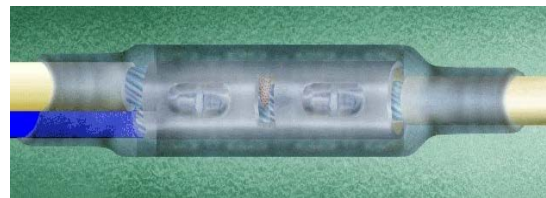


Figure 23: Butt Splice with Heat Shrink

Terminal pins can be either weather sealed, or not weather sealed. Wires with and without a wire seal can be seen in Figure 24 and Figure 25. Terminals being installed in a connector that could come in contact with fluids, connectors in an engine bay, need to be weather sealed. If the terminal will be inside the vehicle and protected from the elements the terminal will not need to be weather sealed.



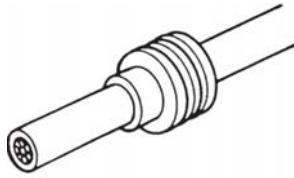


Figure 24: Wire with Weather Seal

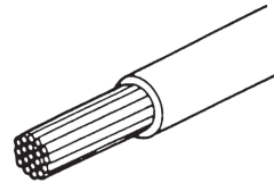


Figure 25: Wire with no Weather Seal

The sealed and unsealed terminals are effectively the same; however, the two tangs, or wings, that grip the insulation of the wire are typically bigger for the sealed terminals. This allows the seal to also be gripped by the tangs. See Figure 27. Just as the butt splice, the manufacturer documentation should be referenced for proper preparation of the wire. Typically a quarter inch of insulation is removed from the conductor. The wire can then be place into the terminal pin to test the fit of the wire. The conductor should pass the core tangs, or wings, by about a millimeter. If there is a little extra length that is fine. The insulation should be the only thing crimped by the insulation tangs. If the conductor is being grabbed the insulation could pull away from the conductor. Once the wire is ready, the terminal pin and wire is crimped together using a proper crimper for the terminal pin. The process for crimping a terminal pin is seen in Figure 26 through Figure 29 [10].

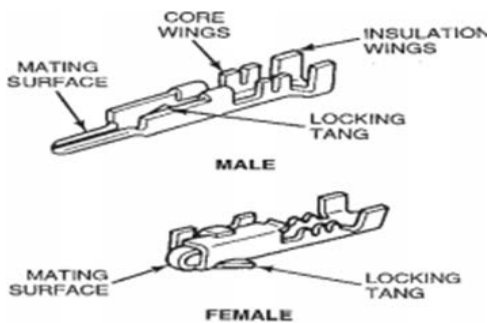


Figure 26: Typical Crimps Terminal Pins

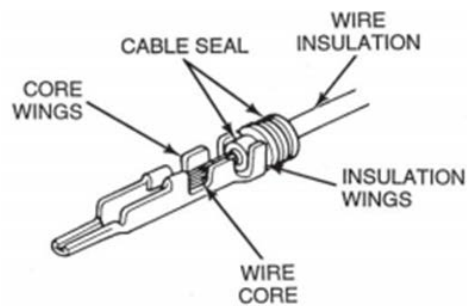


Figure 27: Sealed Terminal

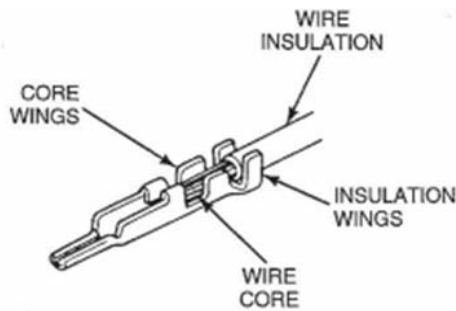


Figure 28: Unsealed Terminal

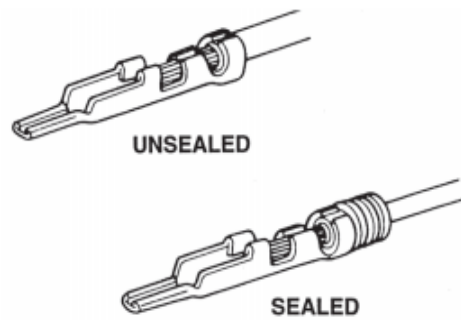


Figure 29: Crimped Terminals

### 7.1.1.3 Wire Preparation

Proper wire stripping tools should be used to remove wire insulation from a conductor. Wire strippers, Figure 30, are machined in such a way that they will not damage either the wire insulation or conductor while using the tool.

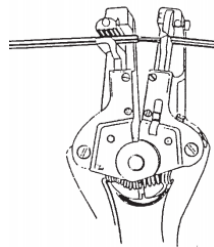


Figure 30: Wire Strippers

After stripping the wire, the remaining insulation should not exhibit any damage such as nicks, cuts, crushing, or charring. [9] Conductors shall also not exhibit any damage. The conductor should not be scraped, bent, nicked, crushed, or cut [9]. Any damage to the conductor will lower the ampacity of the wire, and cause a point of failure. If either the

insulation or conductor is damaged during preparation the end should be cut off and remade. Figure 31 shows a properly made wire end, and Figure 32 through Figure 37 shows ends needing to be remade [11].

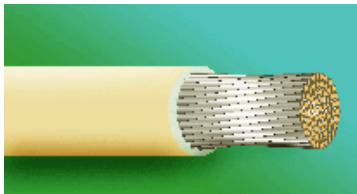


Figure 31: Proper Wire

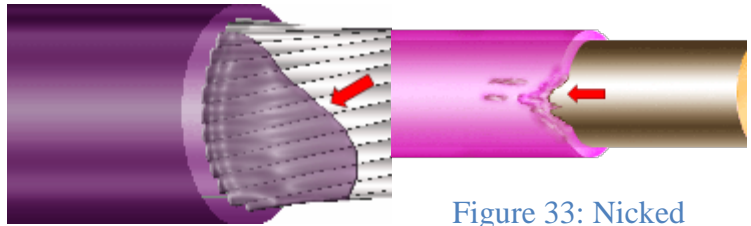


Figure 32: Extra Insulation

Figure 33: Nicked Insulation

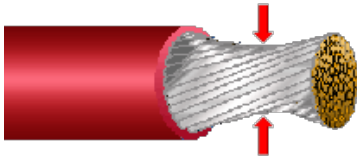


Figure 34: Over twist

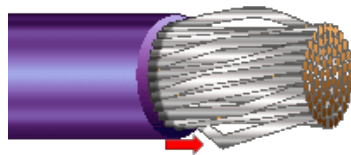


Figure 35: Bent Conductors

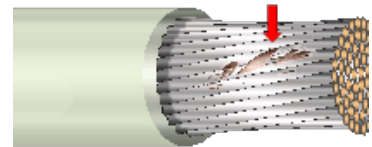


Figure 36: Nicked / Cut Conductors

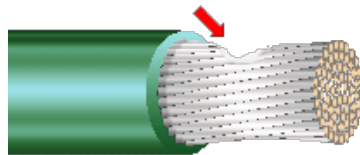


Figure 37: Crushed Conductor

## 7.1.2 Wire Sizing

“Selecting the correct wire gauge ensures the proper voltage supply to an electrical device and prevents the cable from overheating” [10]. A wire can be thought of a long resistor; therefore, resistance and ampacity should be considered when selecting the proper wire gauge. “All electrical conductors have some resistance to the flow of electrical current.

The resistance of a cable increases as the cross sectional area or gauge decreases. Conversely, cables with a larger cross section have less resistance and thus, a higher ampacity. The current in a cable can cause the cable to heat up due to the conductor's (copper) resistance. When current increases to a level high enough to raise the internal conductor temperature to a point that exceeds the maximum temperature rating of the cable, the insulation begins to degrade" [10].

If the insulation degrades to the point of failing the insulation will begin to melt. This will likely result in a short occurring in the circuit causing component malfunction. Also, as current increases in a wire the voltage drop will also increase across the wire. Voltage drop reduces the overall voltage delivered from a supply. Common practices is to have no more than a 2% voltage drop from the power source to a device. For a 14V system, like on a conventional vehicle, the voltage should not fall below 13.72V. For example, a water pump draws 4 amps of current, the total wire length, positive and negative side, is 10 feet, and the wire is an 18 AWG wire. Voltage drop calculation steps given below using Table 1.

- Voltage drop using Ohm's Law:  $V_{drop} = I \cdot R$
- Resistance for 10 ft of 18 AWG wire :  $R = 0.006385 \cdot 10 = .06385 \Omega$
- Current draw of pump:  $I = 4 \text{ A}$
- Voltage drop from wire:  $V_{drop} = 4 \cdot .06385 = .2554 \text{ V}$
- Actual voltage supplied to pump:  $V_{pump} = 14 - .2554 = 13.74 \text{ V}$
- % voltage drop:  $\%V_{drop} = \frac{14 - 13.74}{14} \cdot 100 = 1.86 \%$

A voltage drop of 1.86 % is the end result by using a 10 ft 18 AWG cable to supply the pump with 4 A of current. According to Table 1, an 18 AWG wire can continuously supply 16 A; however, in order to supply the correct voltage to the pump the 18 AWG is

needed. A 22 AWG wire is also able to carry a 4 A draw, but due to the length of the wire the voltage drop will greatly increase. See below calculation.

- Voltage drop using Ohm's Law:  $V_{drop} = I \cdot R$
- Resistance for 10 ft of 22 AWG wire :  $R = 0.01614 \cdot 10 = .16 \Omega$
- Current draw of pump:  $I = 4 \text{ A}$
- Voltage drop from wire:  $V_{drop} = 4 \cdot .16 = .64 \text{ V}$
- Actual voltage supplied to pump:  $V_{pump} = 14 - .64 = 13.36 \text{ V}$
- % voltage drop:  $\%V_{drop} = \frac{14 - 13.36}{14} \cdot 100 = 4.57 \%$

If a 22 AWG is used to power the pump the voltage drop of 4.57 % exceeds the 2 % maximum voltage drop.

Table 1: AWG Wire Table

AWG gauge	Conductor Diameter Inches	Ohms per 1000 ft.	Maximum amps
0000	0.46	0.049	380
000	0.4096	0.0618	328
00	0.3648	0.0779	283
0	0.3249	0.0983	245
2	0.2576	0.1563	181
4	0.2043	0.2485	135
6	0.162	0.3951	101
8	0.1285	0.6282	73
10	0.1019	0.9989	55
12	0.0808	1.588	41
14	0.0641	2.525	32
16	0.0508	4.016	22
18	0.0403	6.385	16
20	0.032	10.15	11
22	0.0254	16.14	7

### 7.1.3 Fusing

“The fuse is a simple and reliable safety device. It is second to none in its ease of application and its ability to protect people and equipment. The fuse is a current-sensitive device. It has a conductor with a reduced cross section (element) normally surrounded by an arc-quenching and heat-conducting material (filler). The entire unit is enclosed in a body fitted with end contacts” [5].

Once the correct wire size has been determined for a given circuit, the wire now needs to be protected from damage, insulation failure from high temperature, for both extended high currents and short circuit current conditions. The proper fusing and wire sizing is the foundation for a safe electrical system. Fuses must be sized to interrupt the flow of current before the conductor reaches its ampacity. Improper fuse sizing can result in dangerous thermal failures in an electrical harness, as wires heat up potentially melting the insulation.

Fuses have specific voltage ratings that should not be exceeded to ensure proper safety. When a fuse blows, it must be able to extinguish the electrical arc in the conduction path in a short amount of time, or current may continue to flow allowing a fault to not be corrected. To accomplish this, general automotive fuses for use in low voltage systems are rated to 32 V. Figure 38 shows fuses typically used for automotive applications.

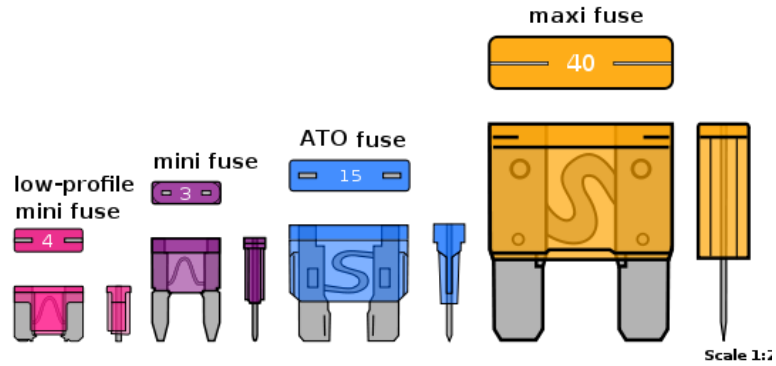


Figure 38: Common Automotive Fuses

When determining the correct fuse for an application one must keep in mind the device being powered is not what the fuse will be protecting. The fuse is protecting the wires. The wire for a given device should be sized to provide the correct current for the device, but is also capable of carrying much more current safely. This is due to adjusting the wire size due to the voltage drop caused by the resistance and length of the wire. What the fuse is protecting is a worst case scenario of a hard fault, or short, in a wire. This can be caused by a wire accidentally being cut, chemical damage of the insulation, or the insulation being worn away by chafing. Whatever the cause of the loss of insulation the bare wire will eventually come into contact with the frame of the vehicle which shorts the wire to ground. At this point the wire has very little resistance and will pull an amount of current greater than the wire can handle. Going from the above example of the pump, an 18 AWG wire at 10 feet has  $0.16 \Omega$  of resistance. At 14 V, for automotive, and  $0.16 \Omega$  the wire will pull close to 88 amps of current. In this case if the fuse doesn't blow the insulation of the wire will completely fail potentially causing damage to the vehicle and/or fire.

Table 2 shows the common amp ratings and color codes for automotive fuses. This standard is used for all manufactures.

Table 2: ATM Cooper Bussmann Automotive Fuses

<b>Product Code Amp rating</b>	<b>Body Color</b>	<b>Voltage Rating DC</b>
ATM-2	Gray	32V
ATM-3	Violet	32V
ATM-4	Pink	32V
ATM-5	Tan	32V
ATM-7 ½	Brown	32V
ATM-10	Red	32V
ATM-15	Light Blue	32V
ATM-20	Yellow	32V
ATM-25	White	32V
ATM-30	Green	32V

Some components in a vehicle will cause an inrush current when turning on. An inrush current is a current that lasts for a short period of time, usually less than a second, just as the device is turning on. It is a much larger current than what is typically drawn during normal operation; therefore, the inrush current should be taken into consideration when sizing a fuse. A fuse blows when the element inside the fuse melts. This is caused by the current heating the element. It is possible to have a fuse carry a current greater than what the fuse is rated for as long as it is for a short period of time. Figure 39 gives the time-current characteristic curves for each automotive fuse. This can be used to ensure a fuse will not blow due to an inrush current.



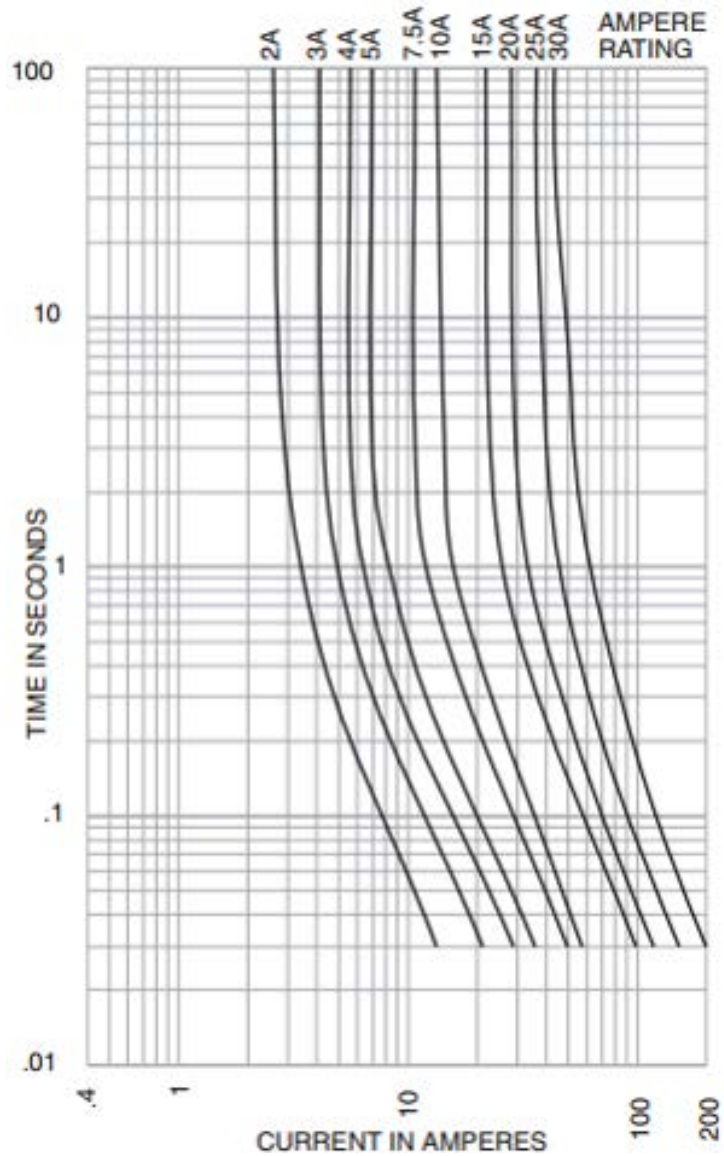


Figure 39: Fuse Time-Current Characteristic Curves

## 7.2 SCR

As emissions regulation become ever stricter there has become a need to reduce emissions of today's vehicles. Diesel engines have an advantage over conventional gasoline engines since they produce 20% less CO<sub>2</sub>; however, diesel engines produce more NO<sub>x</sub> [12]. By 2025 the US EPA is calling for a 75% reduction in NMOG+NO<sub>x</sub>, and Europe

will also be calling for a heavy reduction of NO<sub>x</sub> emissions [13]. To help reduce emissions on the Malibu a Selective Catalytic Reduction (SCR) system is installed on the vehicle's exhaust.

The mechanical team handled the physical mounting of the SCR components, while the electrical team wired everything together. All of the components used in the SCR system, detailed in Figure 40, were sourced from a Chevrolet Cruze. Pinouts of each component were available to the team by using parts from a General Motors vehicle, but datasheets were not supplied. This made it difficult to control both the injector and pump. Testing needed to be completed to properly control each component. Each component was for current draw to properly size power wires. The current draw and wire size for each component is listed in the schematic of Figure 40.

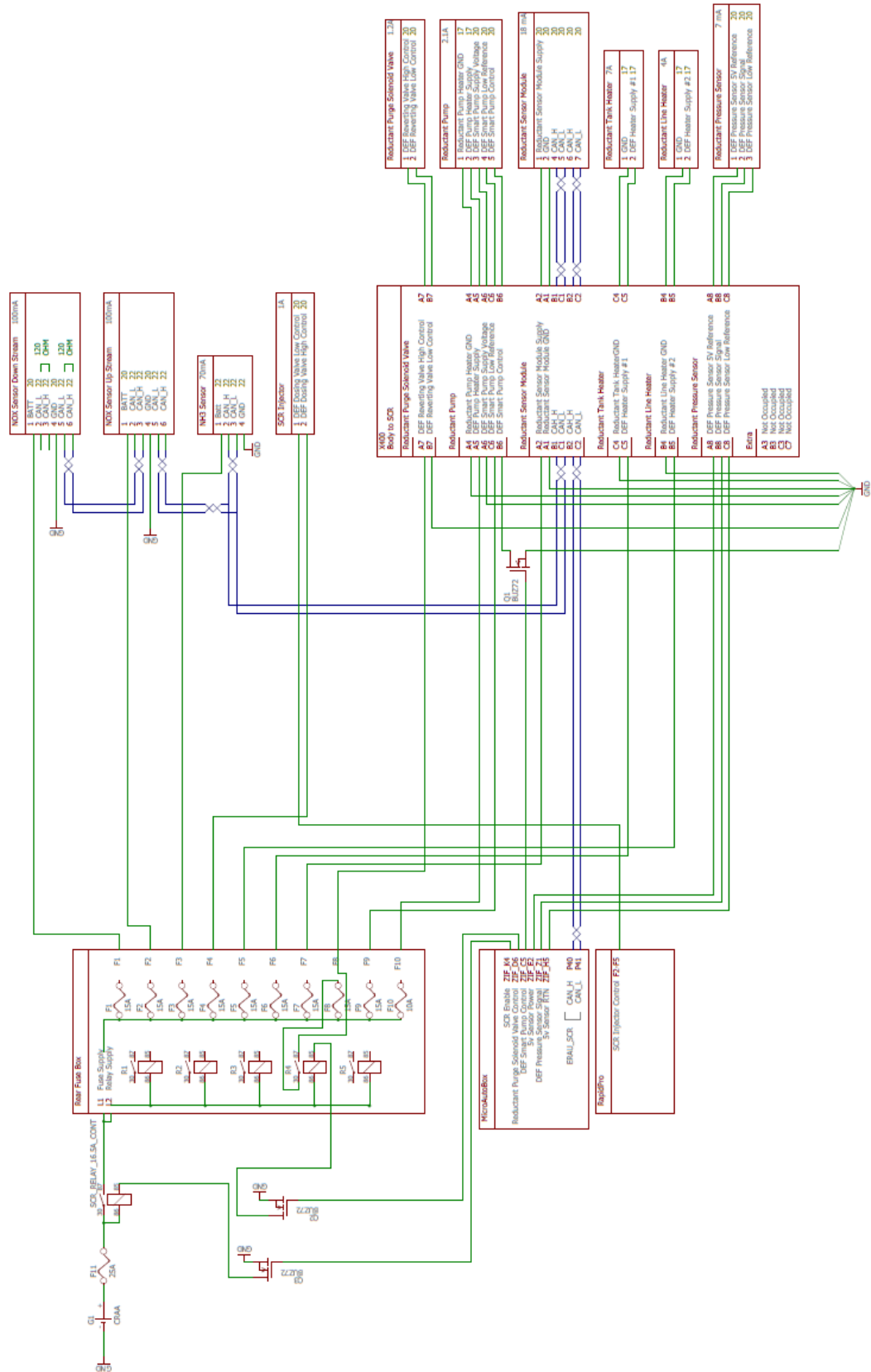


Figure 40: SCR Schematic

## 7.3 Can Bus

A modern vehicle is made up of many different controllers to run the vehicle, and it is often necessary for these controllers to share data with each other. In order to share information a network is formed with controllers called a CAN bus, or Controller Area Network Bus, this type of communication uses two separate wires twisted together to send signals. These wires are called CAN High and CAN Low. Figure 41 shows the signals when viewed on a scope. CAN\_H is from 2.5 V to 3.5 V, and CAN\_L is from 2.5 V to 1.5 V [14]. The CAN system takes the difference between the two voltages to transmit data in binary. In the recessive state of 0 volts the signal represents a binary 1, and in the dominant state the signal will be 2 volts representing a binary 0. Being a twisted pair with a differential type signal, the CAN bus is highly immune to noise. The twisted wires provide noise immunity, but if noise does contaminate the signal it will add contamination to both CAN\_H and CAN\_L. Taking the difference of CAN\_H and CAN\_L will filter out any noise in the signals due to both signals being affected the same [14].

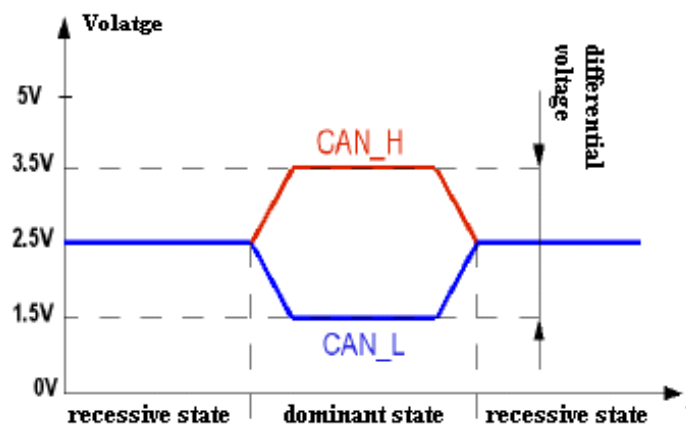


Figure 41: CAN Bus Signals

Figure 42 gives the basic layout of the CAN bus. The bus can have as many nodes, or controllers, as desired in the system. The two main design considerations must be followed. First, there must be terminating resistors of 120 ohms at the far ends of the bus. This matches the impedance across the entire bus to 60 ohms, and ensures the signals on the bus do not degrade [14]. If the terminating resistors are left out a signal will reflect back onto the bus after it has been sent and can corrupt the next message. The second design consideration is to keep the stub lengths from the main bus to each node as short as possible. As the stub length increases the impedance will also increase. If the stub length becomes too great then messages on the bus will begin to reflect back onto the bus causing messages to be lost. Best practice is to keep the stub lengths less than two inches [14].

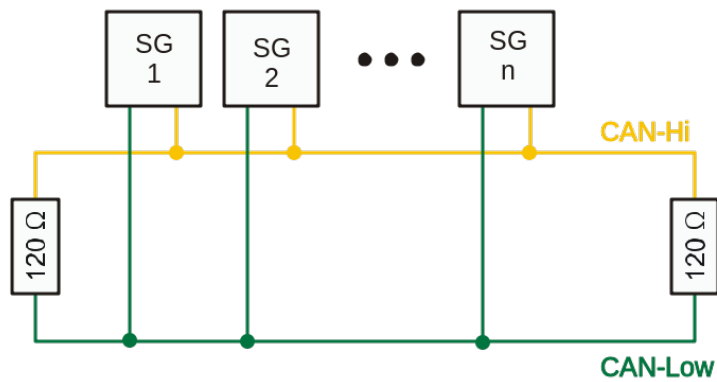


Figure 42: Basic CAN Bus Diagram

## 7.4 HV Charging

By using the J1772 standard, the vehicle is able to charge using a variety of common and accessible electric vehicle supply equipment (EVSE). The two most common ways the

ERAU EcoCAR is charged is by using a portable charger, or a level 2 charging station located on the ERAU campus electric vehicle parking spaces. The portable charger is limited to a common 120 VAC outlet which allows the BRUSA to charge the battery pack at a max of 1 kW. The size of the unit allows it to be carried in the vehicle to allow charging when only a 120 VAC outlet is available. The charging station uses 220 VAC as its voltage input, and this will enable charging up to 3.3 kW with the BRUSA. Table 3 shows the charging characteristics of the BRUSA as well as the approximate charging times of the EVSE used to charge the vehicle.

**Table 3: BRUSA Charging Characteristics**

AC Voltage	Charging Equipment	Output Power	Time to Charge Pack
120 V	Portable	1 kW	~16 hours
220 V	Station	3.3 kW	~5 hours

The BRUSA is controlled over CAN by the Battery Management System (BMS) of the ESS. The BMS sends commands over CAN to the BRUSA for what voltage and current should be outputted to the ESS. The general high level charging procedure is as follows:

1. EVSE cordset plugged into vehicle.
2. BRUSA turns on and wakes up the ESS BMS.
3. BMS requests power, and enables the BRUSA to begin charging.
4. BRUSA follows BMS commands to charge the ESS.

To help initiate the charging process, and add levels of safety, the J1772 standard utilizes Control Pilot (CP) and Proximity circuits. Figure 43 shows the CP and Proximity

circuits detailed in the J1772 standard. The Proximity circuit is used to ensure the vehicle cannot drive while the vehicle is plugged into an EVSE. This is solely for safety. CP has two functions. The first is also a safety feature where the EVSE is signaled it is safe to provide power to the vehicle. The second feature of CP is to signal the vehicle what the max current limit the EVSE is able to supply. This keeps the BRUSA from pulling too much current from the EVSE. A more detailed explanation of the CP function will be given in the Results section.

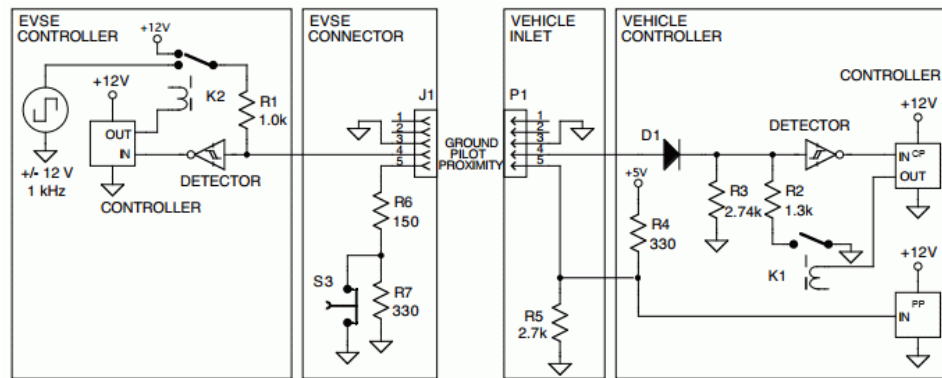
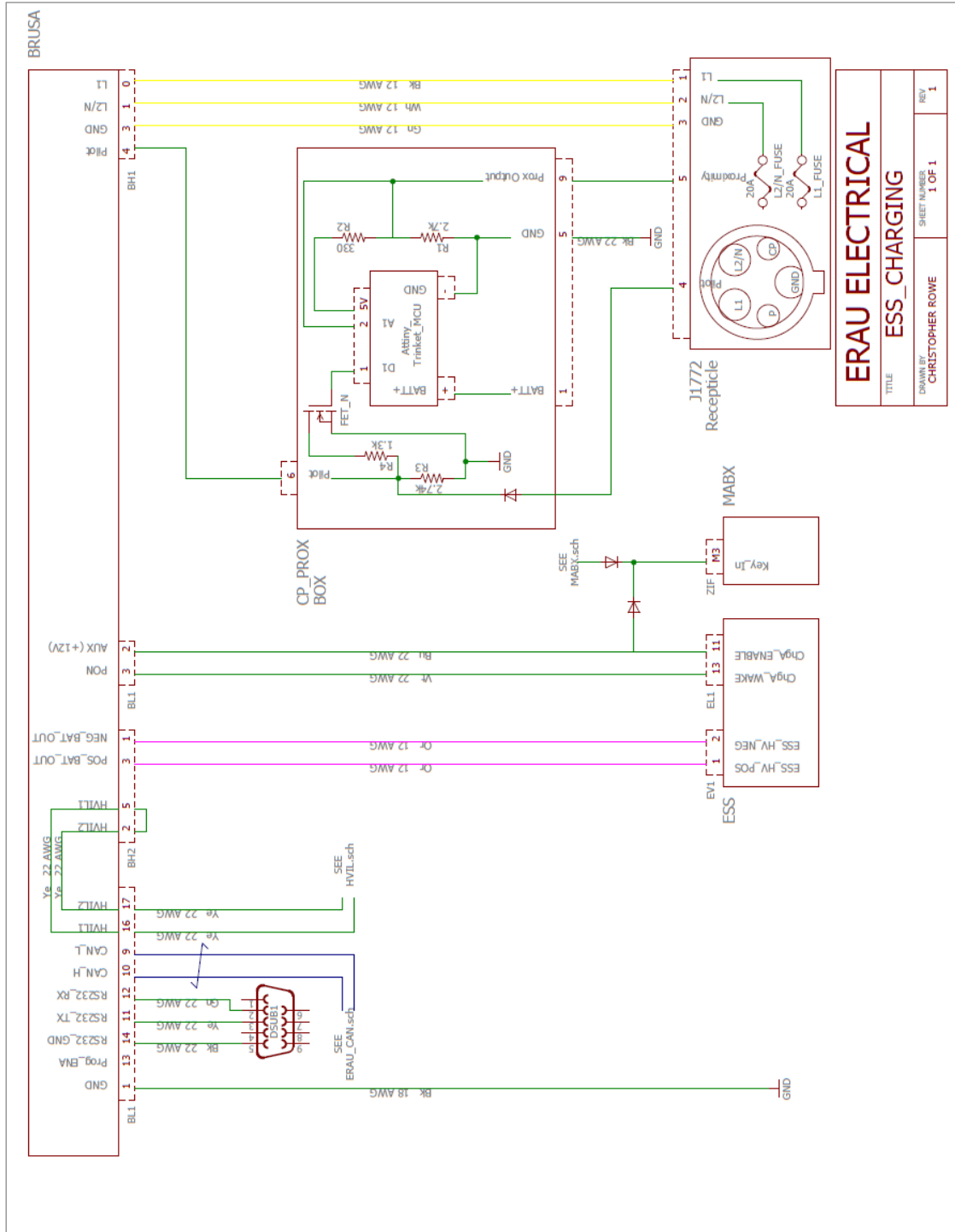


Figure 43: J1772 Schematic [15]

The schematic designed for the charging system is shown in Figure 44 shown below.



<b>ERAU ELECTRICAL</b>	
TITLE <b>ESS_CHARGING</b>	
DRAWN BY CHRISTOPHER ROWE	SHEET NUMBER 1 OF 1
REV 1	

Figure 44: Charging Schematic



## 7.5 GM vs. ERAU Drive Testing Procedure

Two separate tests have been performed on the vehicle. The first test was performed at the General Motors (GM) Milford proving grounds facility. Testing was conducted by GM-approved test-track drivers, and they followed a drive schedule to mimic a mix of highway and in-city driving. During the GM testing, the vehicle pulled a small utility trailer equipped with a SEMTECH DS exhaust emission analyzer. This equipment was used to gather emissions data from the vehicle throughout the length of the test. Regenerative braking was not used during the GM testing. Regenerative braking was intended to be used; however, it was disabled by accident and the test could not be re-run.

The second test was performed by ERAU-approved drivers on the EcoCAR team. The vehicle was driven on city roads and on the highway to gather the needed data. Due to instrumentation limitations, emissions data could not be gathered from the vehicle while testing. Regenerative braking was fully enabled during the ERAU testing. It is important to note that the GM test was done overnight for 5.5 hours. Due to student schedules, the ERAU test could only be performed for a little over 2 hours.

For both tests, prior to testing, the vehicle's ESS is fully charged/balanced and the fuel tank is filled. The tank is filled by removing the tank from the vehicle enabling the tank to be weighed. This gives a more precise approximation for fuel consumed while operating the diesel generator. The vehicle drive cycle is then carried out. Once testing is completed the vehicle is returned to the garage where the fuel tank is removed from the

vehicle for weighing in order to find the total fuel consumed during testing. Lastly, the vehicles ESS is charged back to 100% SOC.

Simulations have shown that a 10% reduction in drag will result in approximately a 6% decrease in energy consumption for a majority of drive cycles [16]. The vehicle has been outfitted with a side-skirting system which will reduce the amount of air spilling out from the sides of the vehicle underbody. This reduction in spillage will energize the flow underneath the vehicle and further reduce drag. This will be accomplished with the use of nylon bristles that act as a weather guard. This will allow a close proximity with the ground for improved aerodynamics without sacrificing ground clearance. CFD simulations have shown an approximate 5% reduction in drag. To increase the skirting system's effectiveness, the vehicle will also implement aerodynamic wheel covers [17]. These have shown significant reductions in drag in previous research [18]. These, like the skirting system, act to reduce the amount of air spilling from the underbody of the vehicle. Since the vehicle has regenerative braking, reductions in brake cooling are negated. Finally, vortex generators which act to reduce flow separation on the rear window are installed on the vehicle [17]. Figure 45 shows the aerodynamic modifications installed on the vehicle [2].



Figure 45: Aerodynamic Modifications

## 7.6 HV Distribution Box

### 7.6.1 Demo Box Constraints

To aid the team in component calibration and testing for EcoCAR 3. A HV demo box has been designed specifically for bench testing of HV components within the lab. The demo box will also serve as a tool to teach students HV safety and good practices.

Table 4: HV demo box constraints

Temperature (due to enclosure)	-20 to 80°C
Continuous Current	125A
Maximum Operate Voltage	400V
Ingress protection	Minimum of IP66/67
Impact resistance	IK08/IK09
All materials resistant to automotive fluids	Yes
Electrical insulation	Totally insulated

## 7.6.2 Demo Box Basic Design

The general HV layout is shown below in Figure 46. The design was kept as simple as possible to aid in component management; such as, wire bend radius. The 2/0 Cable has a bend radius of 4.5 in. If a bend was attempted inside of the demo box much of the space will be wasted. Due to this fact, the HV cables were kept straight to maximize the space in the box. Another important detail to note is that the extra space was utilized by making it possible to expand the HV circuitry. This is seen in Figure 46 where there is extra space for a HV fuse, lugs on the positive buss bar, and space for another lug on the negative buss bar.

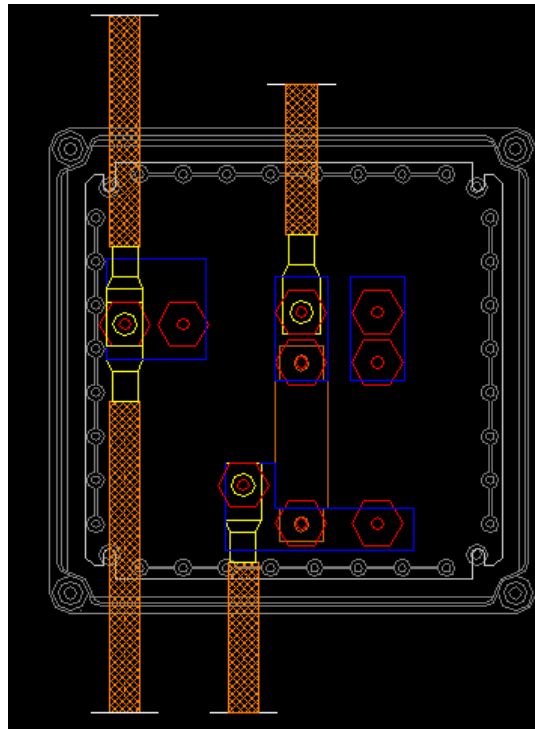


Figure 46: 2D CAD Drawing

### 7.6.3 Block Diagram

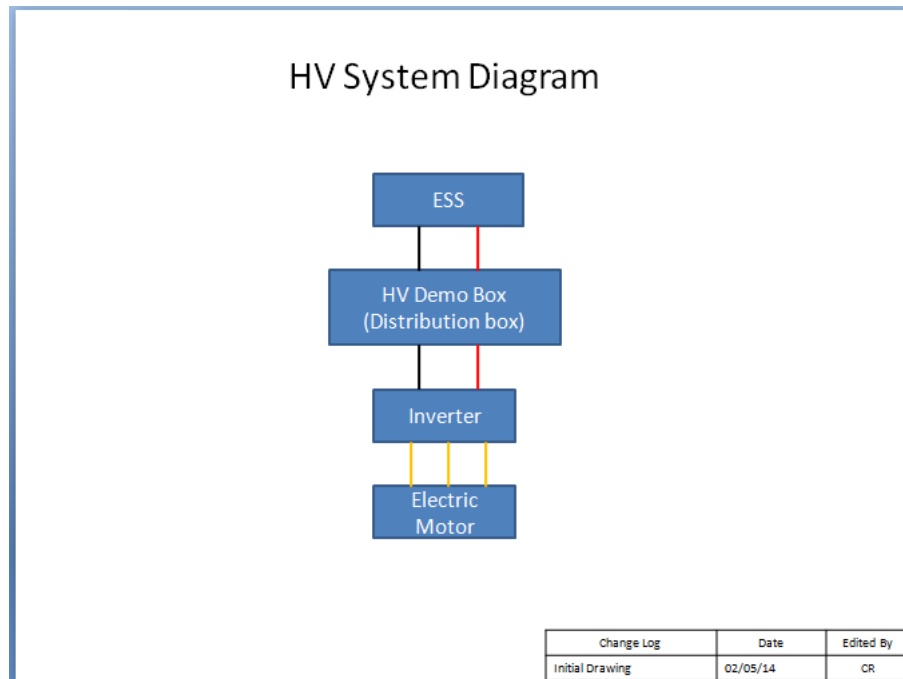


Figure 47: HV Demo Box Block Diagram

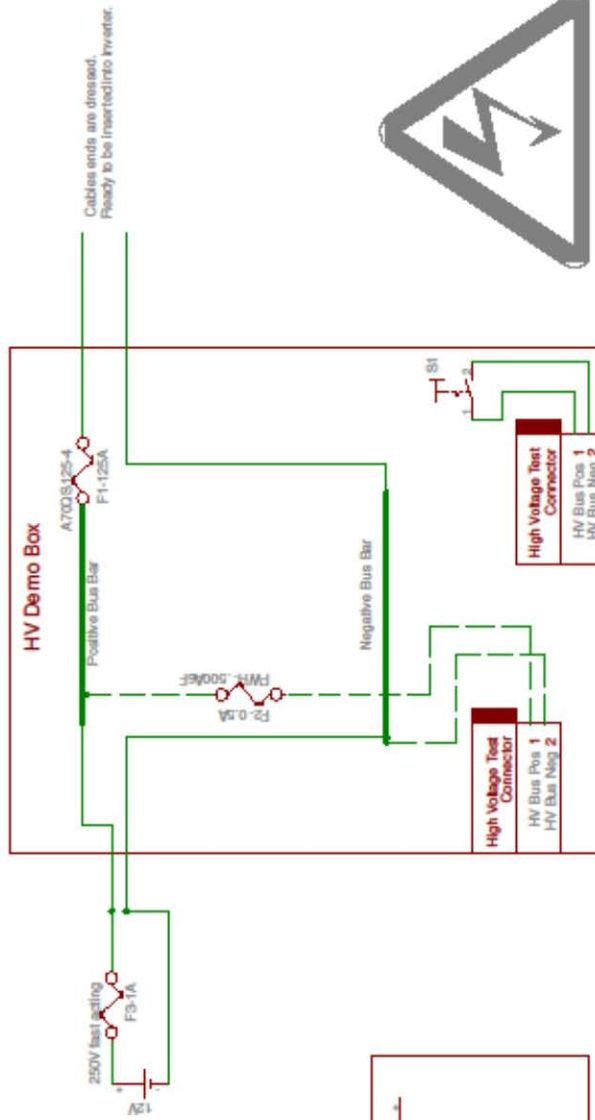
## 7.6.4 Schematic

### HV Demo Schematic

Change Log	Date	By
Initial drawing	02/05/2015	CR
Updated to "as-built"	02/09/2015	CR

Logic used on Busbar	Wire Size
Burndy YAG2L	20AWG
T&B 25e-30695-131	20AWG
Ring Terminal	18AWG



Legend	
18 AWG, HV	Battery
20 AWG, HV	
Cu Bus Bar, HV	
20 AWG, LV	
Fuse	

et: 1/1)

Author: Chris Rowe  
Date: Feb-09-2015  
Rev: 2

## 7.6.5 HV Fusing

The “High Speed Fuse Application guide” document by Cooper Bussmann was utilized to find the proper fuse rating. The HV fuse de-rating scheme used is given below. This calculation will be used to size the fuse for the PM100DX inverter to run a REMY HVH250-S generator.

$$I_b = I_n * K_t * K_e * K_v * K_f * K_a * K_b$$

$$I_b = 125 * 1 * 1 * 1 * 0.60 * 1 * 0.80 = 60 \text{ A}$$

**I<sub>b</sub>**: Max cont. load current

**I<sub>n</sub>**: Rated fuse current. For PM100DX I<sub>n</sub>= 125

**K<sub>t</sub>**: Ambient temperature correction factor, room temp, K<sub>t</sub>=1.00

**K<sub>e</sub>**: Thermal correction factor, 1.3 amp/mm<sup>2</sup>. K<sub>e</sub> = 1.00

**K<sub>v</sub>**: Cooling air correction factor, mounted in box w/ no air flow, K<sub>v</sub>=1.00

**K<sub>f</sub>**: Frequency correction factor, switching frequency of 12kHz, K<sub>f</sub>=0.60

**K<sub>a</sub>**: Correction for altitude, primarily under 2000m, K<sub>a</sub>=1.00

**K<sub>b</sub>**: Fuse load constant, fiber bodied fuses, K<sub>b</sub>=0.80

After this calculation, it can be seen that a 125A fuse will be good for 60A continuous after the derating is applied. The fuse chosen for this application is the A70QS125-4. This fuse is rated for 125A at up to 700V DC, and Figure 48 shows the fuse curve for this series.

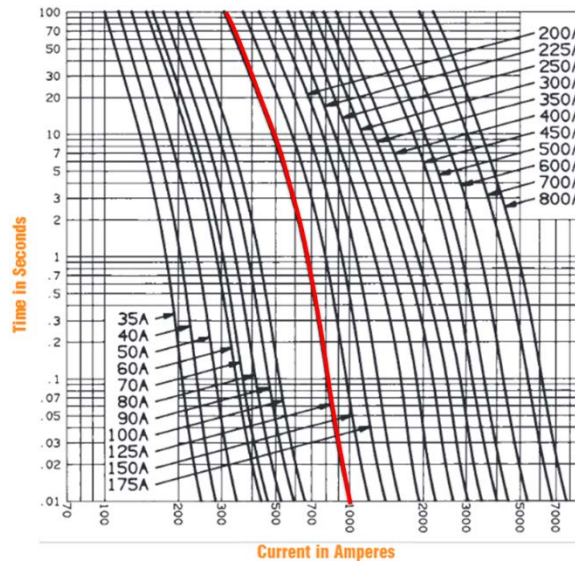


Figure 48: HV Fuse Curve

### 7.6.6 HV Test Connector Fusing

For safety and good practice, .5A fuses (FWH-.500A6F) were placed in the circuits of the positive and negative conductors of the HV test connector. This fuse is rated up to 500V.

### 7.6.7 Torque Specifications

The only hardware needed to be torqued for the HV demo box are currently only bolts. Table 5 shows the bolt specifications as well as the required torque. All other hardware used in the HV demo box does not specify a torque. These items include: Cable glands, fuse holder, and HVIL connector. These items were tightened till snug and then turned an extra quarter turn to ensure they are secure.



Table 5: Bolt Torque Specs

Length (mm)	Type	Material	Grade	Torque (Nm)
12	M6-1.0	Zinc-Plated Steel	8.8	11
16	M6-1.0	Zinc-Plated Steel	8.8	11
20	M6-1.0	Zinc-Plated Steel	8.8	11
25	M6-1.0	Zinc-Plated Steel	8.8	11

## 7.7 HV Simulation

In order to estimate the voltage ripple and resonant frequency on the HV bus a simulation model was created. This model, seen in Figure 49, includes four subsystems to model the dynamics of the bus. These systems are the HV battery, BRUSA, HVAC (High Voltage Air Conditioning), traction motor, and generator. To create this model Matlab and Simulink were utilized. The blockset specifically used in Simulink is the Electrical Simscape blockset. This allowed simple modeling of a complicated system, and did not need each component of the system fully characterized. The main focus of this simulation is to estimate the voltage ripple and resonant frequency on the main HV bus. The voltage ripple is caused by the switching characteristics associated with the inverters converting DC to AC power to drive the electric IMG motors. The resonant frequency is biased by the electrical characteristics, inductance and capacitance are the main sources, of each component and HV cables. The goal is to calculate the resistance, inductance, and capacitance of the HV cabling using a Matlab script that can be used in the model. These characteristics and the components are then used to simulate the voltage ripple and resonant frequency.

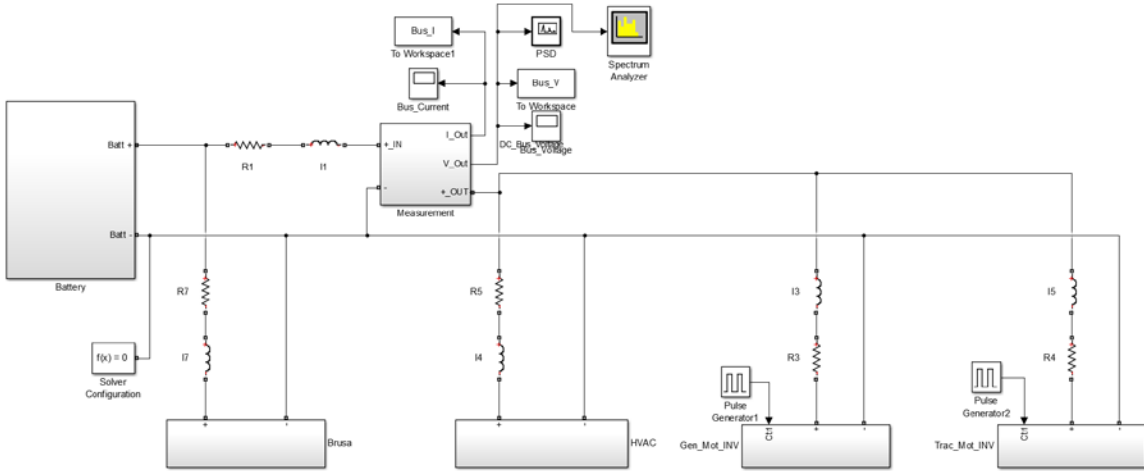


Figure 49: HV Simulation Simulink Model

To collect data from the simulation, Figure 50, the Power Spectrum Density (PSD) and Spectrum Analyzer blocks were used. The PSD block is used to find the voltage ripple at specific frequencies, and the spectrum analyzer is used to find the resonant frequency and harmonics. Bus voltage and current are also recorded for use in post processing. The measurement subsystem uses Simscape conversion blocks to convert the physical signals, used for the model, to Simulink signals. This is necessary due to the fact that Simulink signals are needed for any post processing.

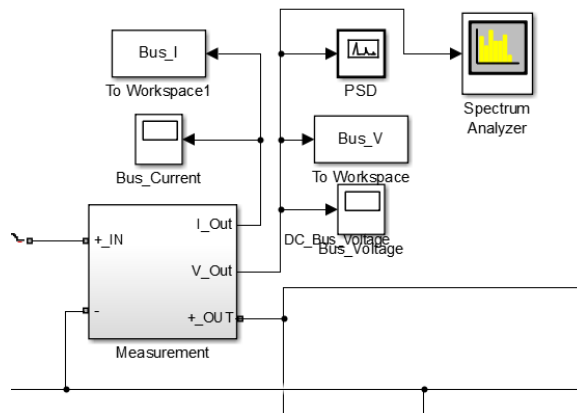


Figure 50: Model Measurements

Figure 51 uses a battery model taken from “Introduction to Hybrid Vehicle System Modeling and Control” by Wei Liu [4]. This Subsystem is used to properly model the ESS characteristics by using the values from Table 6. These values were gathered from “Hybrid electric power system validation through parameter optimization” by Hasnaa Khalifi [19]. This thesis focused on characterizing the battery modules used in the vehicles ESS; however, this thesis is based on an ESS composed of six modules, and the new ESS being designed for EcoCAR 3 will have seven modules. To aid the team in characterizing the ESS modules, the University of Washington’s EcoCAR 3 team also provided some information on the module characteristics since they have previously used seven modules in EcoCAR 2.

Table 6: ESS Battery Characteristics

<b>Component</b>	<b>Value</b>
V Open Circuit	350.000 V
Ro	0.050 $\Omega$
Cep	1294.000 F
Ccp	525.200 F
Cep Resistor	.002 $\Omega$
Ccp Resistor	.080 $\Omega$

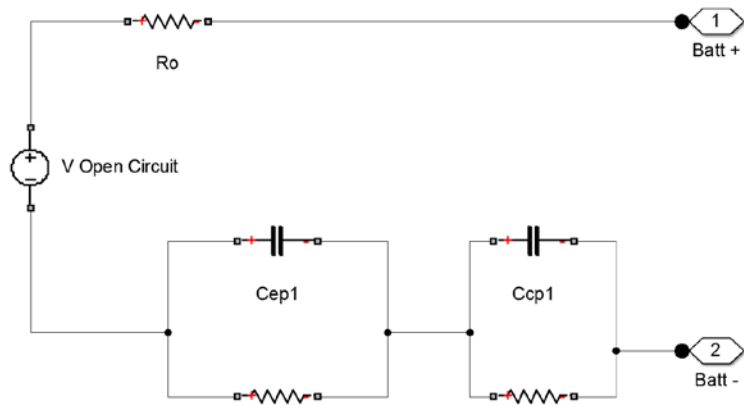


Figure 51: ESS Battery Subsystem

Figure 52 shows the subsystem system used to model the high voltage air conditioner in the vehicle. The DC Current source is used to insert a 16 amp draw on the high voltage bus. 16 amps was chosen since 16 amps is the max current that will be drawn by the device.

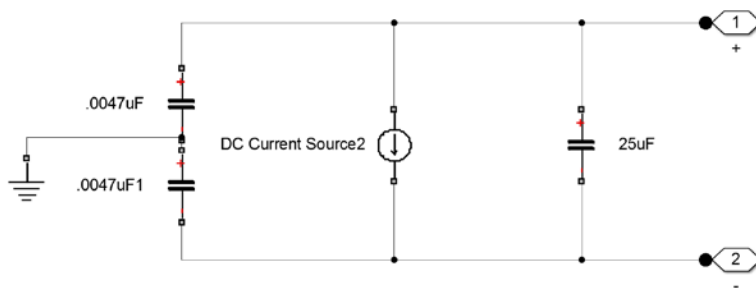


Figure 52: HVAC Subsystem

Figure 53 shows the subsystem used to model the BRUSA battery charger. The BRUSA is not on during normal vehicle operation. This makes it a passive device on the bus, and it only adds capacitance, 8uF, from its bulk capacitor to the system.

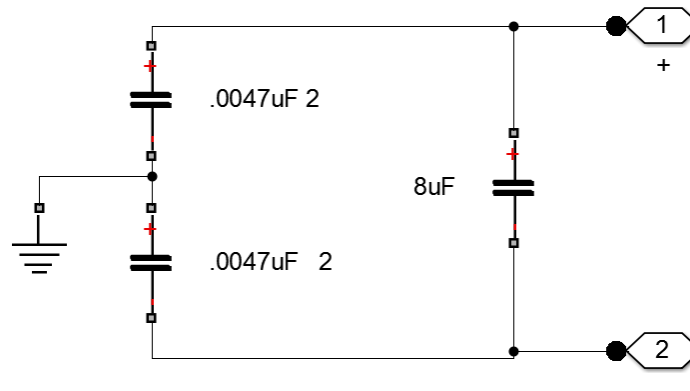


Figure 53: BRUSA Subsystem

Figure 54 shows the subsystem used to model the inverters used in the vehicle. This subsystem is used for both the traction motor and generator. The goal is not to model all the characteristics of the inverter; instead, the higher level function is modeled. This function is the high frequency switching needed to create AC power from the high voltage DC bus. This is needed since the electric motors are AC three phase motors. Typical switching for AC inverters is anywhere from 1 kHz to 12 kHz. A current source controlled by a pulse generator is used to induce a 300 amp current draw at a frequency specified in the pulse generator. By adjusting the frequency of the pulse generator post processing can be done to find the voltage ripple and resonant frequency on the bus.

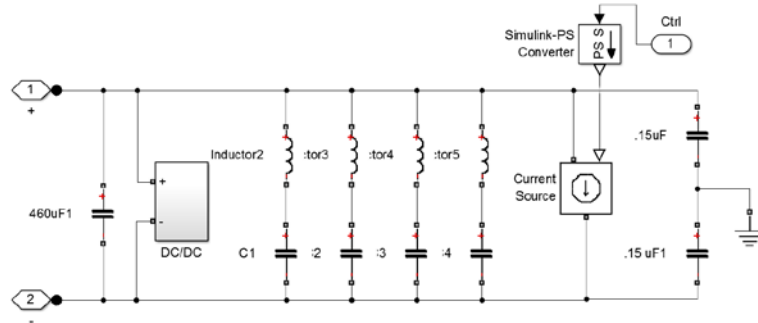


Figure 54: Inverter Subsystem

Figure 55 shows the subsystem used to model the DC/DC converter, or APM, this is housed in the inverters. The DC/DC converter is used to provide low voltage, 12 – 14 V, power to keep the 12 V battery charged and power vehicle systems.

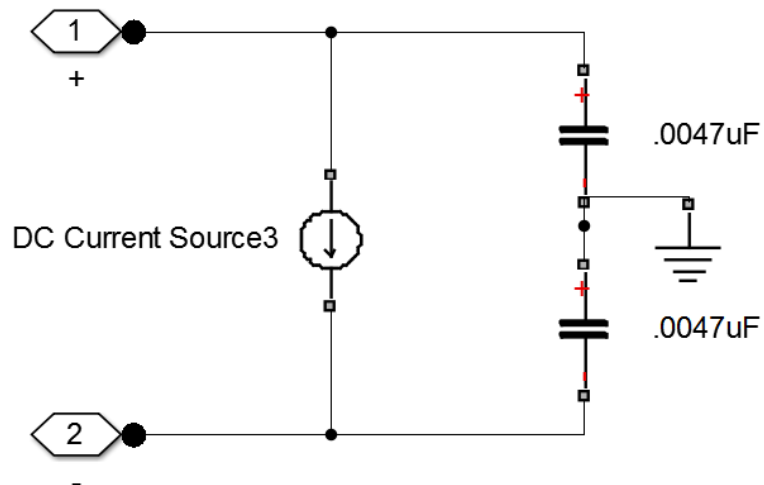


Figure 55: DC/DC Subsystem

## 8. Results

### 8.1 Vehicle Wiring

#### 8.1.1 Low Voltage

At the end of EcoCAR 2 Y2 the vehicle was electrically in very bad shape. The HV systems were in the vehicle, and for the most part in good working order. The low voltage systems were not in good shape. The vehicle could not spin the wheels, the engine was never wired, an SCR system was not even designed, the ESS was not capable of being charged, and there were numerous wiring mistakes throughout the vehicle.

Beginning EcoCAR 2 Y3, the vehicle systems were meticulously gone through to root out any issues. Two common issues were found to be the main problem for the vehicle. The first issue was bad crimping and soldering techniques were used. Figure 56 though Figure 58 shows example of bad crimps. Bent crimps made it difficult to seat the pin in a connector, and often the pin would not lock into the connector. If the pin cannot lock it will eventually fall out of the connector. If the insulation of the crimp is crushed, the copper conductors are weakened and tend to begin to break. Once this happens an intermittent connection forms. This can make it very hard to diagnose a fault in the wiring.



Figure 56: Bad Crimp w/ Insulation Crushed

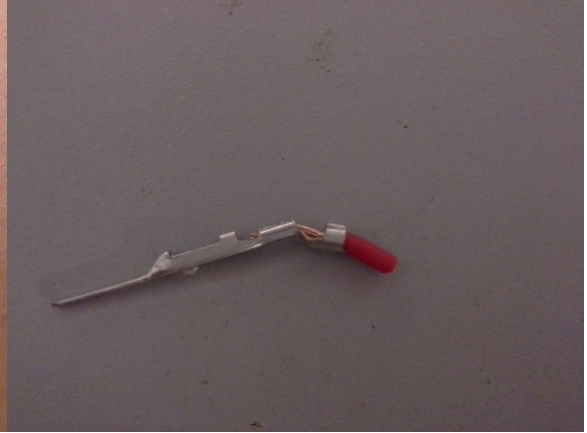


Figure 57: Bent Crimp



Figure 58: Lack of Conductor in Crimp

Bad solder joints often came apart, or even break. If improper soldering techniques are used the solder will not flow correctly. This will cause a cold joint. This cold joint will be dull in color and have cracks in the solder. This will eventually break apart. The solder can also simply sit on top of the wire and not form a proper bond. This will cause the joint to separate.

The second major issue noted throughout the vehicle was wrong wire sizing. Instead of properly sizing a wire for a given circuit, the entire vehicle was wired using 18



AWG wire for the LV systems. The wires should have followed proper techniques to size each wire. This begins with finding the current that will flow through the wire, selecting a wire capable of carrying the needed current, and then making sure the voltage drop of the wire is not more than 2%. If the voltage drop exceeds 2% the wire gauge is adjusted to meet this rule. As an example of this, signal wires running from the vehicle controller were changed from 18 to 22 AWG wires. The signal wires do not carry any current, and the vehicle controller connector was not meant to have 18 AWG wires installed. This caused the wires to become stuck in the connector, made the harness larger than needed to be, and added extra weight to the vehicle.

By using the inverters in CAN mode it was discovered that the inverter only requires 12V wiring to be installed as configuration 0 as seen in Figure 59. The vehicle is currently wired utilizing configuration 1 as seen in Figure 60. Configuration 1 is mainly used in VSM mode where the inverter is the main controller, independent from other systems in the vehicle, used in a vehicle for propulsion. The circuits not needed to implement configuration 0 will be removed, and the inverters will be tested to ensure proper functionality. This refinement has been implemented, and the inverters are working as intended.

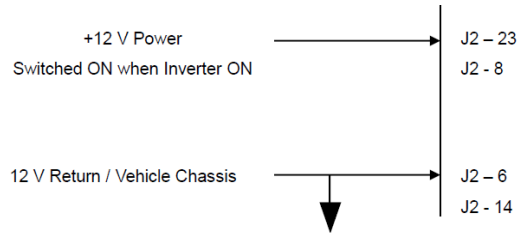


Figure 59: Inverter Configuration 0 Wiring

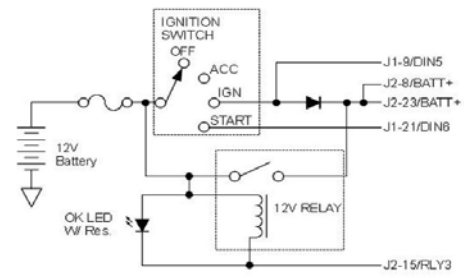


Figure 60: Inverter Configuration 1 Wiring

In order to house the 12V main distribution and disconnect switch a box was made. Figure 61 shows the new box installed in to the vehicle. Fuses for the APM, engine bay fuse box, and interior fuse box are housed inside of the box. The 12V disconnect switch was mounted to the top cover and sealed with RTV to ensure the box is water proof. Figure 62 shows how the components are housed inside the box. This new design made it possible to separate both the 12V battery and APM from the vehicle fuse box. By doing this, the 12V disconnect switch can be turned off, and the vehicle will not have any power sources. The car is sure to stay off when it needs to be off.



Figure 61: New 12V Distribution



5

Figure 62: Inside 12V Distribution Box

### 8.1.2 High Voltage

Unlike the low voltage systems on the vehicle, the high voltage bus was in good working order at the start of EcoCAR 2 Y3. Figure 63 shows the Block Diagram for the HV bus. The layout is relatively simple. The ESS powers all of the components on the bus, and there are two enclosures that allow parallel circuits to branch off from the main HV bus. The first enclosure is the Rear DDE (Distribution and Disconnect Enclosure). The Rear DDE is located underneath the vehicle between the rear wheels. It allows the APM and BRUSA charger to be connected to the main bus. The APM acts as the alternator of the vehicle by converting the HV to LV in order to maintain the 12V battery, and supply power to the LV vehicle systems. The BRUSA is used to charge the ESS, and will be discussed later in this paper. From the Rear DDE the main bus continues on to the Front DDE. This is where the bus gives power to the HVAC (High Voltage Air Conditioning), Traction Inverter, and Generator Inverter. The HVAC uses an electric compressor which allows the vehicle cabin to be cooled without the need of an engine to be running. The Traction and Generator inverters are functionally equivalent. The inverters allow for

bidirectional power flow between the HV bus and the electric Traction Motor and Generator.

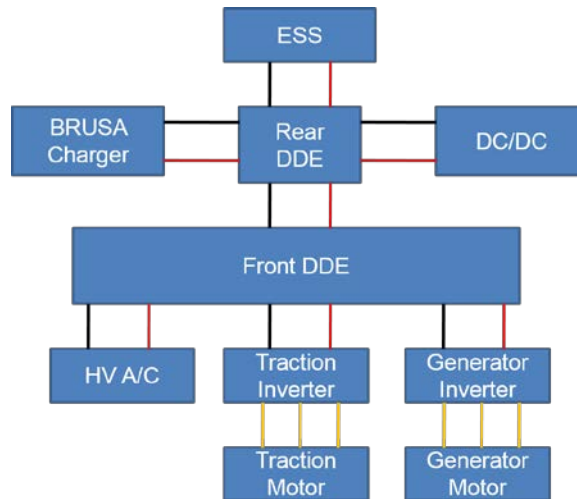


Figure 63: HV Block Diagram

In order to improve the HV bus, some modifications needed to be performed. The work performed included removing excess cable length the engine bay, rerouting HV cables for better fitment, installing new sleeving on the cables, and exchanging the traction motor and generator.

### 8.1.2.1 Cable Length Reduction and re-routing

The HV cables in the engine bay of the vehicle, as seen in Figure 64, needed to be reduced in length and re-routed. This allowed the HV cables to not interfere with the engine or the hood when it is closed. About 2.5 feet of HV cable was removed from each branch leaving the front DDE. Figure 65 shows the HV cables after they were reduced in length.



Figure 64: HV Before Length Reduction



Figure 65: HV After Length Reduction

The cables were shortened at the front DDE, Figure 66, due to the complexity of making the cable ends used to connect into the inverters. The cables were removed from the front DDE, cables cut to proper length, and then reinstalled into the front DDE. This procedure had to be done for both the positive and negative cables



Figure 66: Inside Front DDE

It was also necessary to adjust the length and routing of the three phase cables from the inverters to the electric motors. The generator motor's glands were located next to the

frame of the vehicle. The old routing had the cables pulled tight at the glands causing stress on the cables. The direction of the cables were up towards the front of the vehicle. This direction caused the cables to come into contact with the frame allowing for zero clearance. To rectify this problem, the length of the cables were increased. This allowed the cables to leave the gland, start in a direction downwards towards the rear of the engine bay, and then loop back up towards the front of the vehicle. This loop allowed the cables to clear the frame, and also provided enough slack to remove the stress on the cables.

The traction motor cables also required re-routing, but the cable length did not need to be changed. This was a simple task of changing the paths of the cables slightly to avoid brake lines at the master brake cylinder.

#### 8.1.2.2 Cable Sleeving

A spark-resistant high-temperature fiberglass sleeving with a silicone rubber coating was installed on the HV cables. This sleeving not only protects the cables but also resists fire, hydraulic fluids, fuels, lubricating oils, and its temperature range is  $-65^{\circ}$  to  $+500^{\circ}$ F. Figure 67, Figure 68, Figure 69, and Figure 70 show a sample of the sleeving.



Figure 67: HV Cable Sleeving Test



Figure 68: HV Cable, Med. Force, 10 reps



Figure 69: Sleeving, Med. Force, 10 reps



Figure 70: Sleeving, Heavy Force, Until Failure

A test was conducted to see how the sleeving will hold up when exposed to sharp objects while covering an old HV cable. A large piece of aluminum with an abrasive edge was used to scrape the cable and sleeving against. The cable was ripped apart rather easily to the last layer of insulation, Figure 68, in about six seconds. When the sleeving was scraped in the same manner, Figure 69, for about ten seconds it was evident that the sleeving performed very well. A few nicks made it through the silicone layer, but there was no damage to the fiberglass or HV cable. A final test was performed to test the sleeving until failure. Heavy pressure was applied to the sleeving, Figure 70, for roughly fifteen seconds. The sleeving was shredded exposing the HV cable. The outer layer of the HV cable was slightly ripped while the integrity of the HV shielding was maintained.

The sleeving detailed above was installed on the HV cables in the engine bay. Figure 64 shows the HV wiring before the HV wire reduction and Figure 65 shows the HV wires after.

### 8.1.2.3 Switch Traction Motor and Generator

While performing emissions testing at an EcoCAR 2 event, a discovery was made. This discovery was that our traction motor and generator were switched. Our traction motor

was working as the generator, and the generator was working as the traction motor. While switching them back to their proper places another discovery was made. The gland inserts installed in the true traction motor were a previous revision for this type motor. The difference between the old revision and current glands for the traction motor were simply the size of the gland opening. The older revision had much smaller glands and would only accept a max of a 1 AWG cable. A 1/0 cable had to be used to carry the current to get the performance the vehicle needed to achieve. Figure 71 shows the traction motor with the rear cover removed. The glands were enlarged using reamers to remove excess material from the glands. Once enough material was removed from the glands, to allow for proper cable fitment, the traction motor was re-installed into the vehicle.



Figure 71: Traction Motor with Gland Plate Removed

While switching the motors another discovery came to light for the generator cables. The cable ends had been found to be improperly made. When the ends were made, the shielding of the cables were left to close to the copper conductors with no separating insulation. This made it possible for the shielding to come in contact with the conductors



causing a ground fault to occur. The cable ends were re-made by removing excess shielding, and the heat shrink was added to add proper separation.

## 8.2 SCR

The SCR system is composed of a power distribution box (Figure 75), 2 NO<sub>x</sub> sensors, an NH<sub>3</sub> sensor (Figure 72), Injector (Figure 74), Pump, tank (Figure 73), body to harness connector, and various heaters. Both power and signal wires traveled from the power distribution box to the SCR main connector. This connector, Figure 73, made it possible to easily remove the SCR harness from the vehicle as needed.



Figure 72: NH<sub>3</sub> Sensor



Figure 73: SCR Tank and Body to SCR Harness Connector

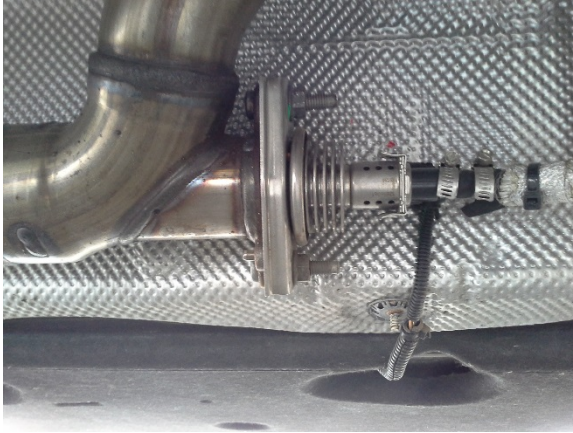


Figure 74: NH<sub>3</sub> Injector

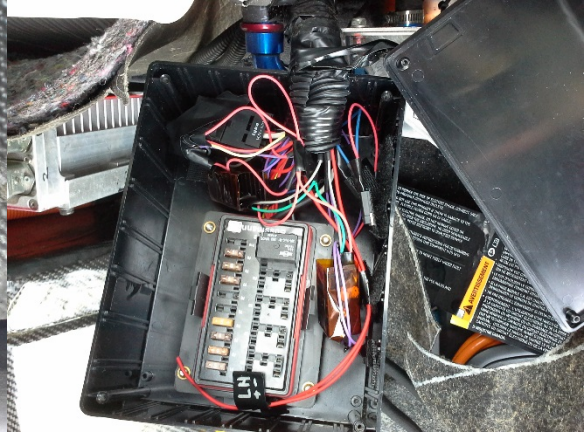


Figure 75: SCR Power Distribution Box

Testing was performed to determine the proper control of the injector and pump. The injector is switched using a low side driver output on the ground wire to turn the injector on or off. For longevity of the injector it was found that the switching frequency of the injector could not exceed 3 hertz. The injector was set to switch at 1 Hz with a 50% duty cycle. These settings gave the best results for injecting the SCR fluid into the exhaust. The duty cycle could be adjusted to change the dosing amount as needed. The pump had a power and ground supply at all times; however, an enable pin had to be driven to control the pump. This enable pin was switched to ground using an n-channel mosfet driven by a pulse width modulated signal. A 100 Hz PWM signal was found to allow the pump to run, while the duty cycle was set to 50%. The speed of the pump could be increased to maintain a certain psi by increasing the duty cycle.

The main controller for the vehicle, MABX, was used to control the SCR system. The RapidPro, a power switching device, had run out of outputs allowing only the injector to be controlled by it. The heaters could be hard wired to turn on when the SCR is on; however, the pump and a few other components still needed to be controlled. To rectify

this issue, digital outputs from the MABX were used to drive n-channel mosfets to control the pump, main SCR relay, and purge solenoid valve in the pump. The digital output could be driven as a PWM or a strait on/off signal as needed for each device.

### 8.3 Can Bus

To rectify errors on the ERAU CAN, the bus was completely re-designed and installed in the vehicle. Figure 76 shows the design of the old ERAU CAN, and Figure 77 shows the team's new design. The new design revision virtually eliminated errors from lost frames occurring on the CAN bus. In order to further improve the robustness of the ERAU CAN bus, individual can message transmission rates were adjusted. Originally, messages were being sent as fast as possible. This causes the bus to be fully utilized to nearly 100% bus capacity; however, this can cause messages to be missed by controllers in the vehicle. By reducing the rates of messages to OEM specifications bus utilization on the ERAU CAN was able to be reduced to 60%.

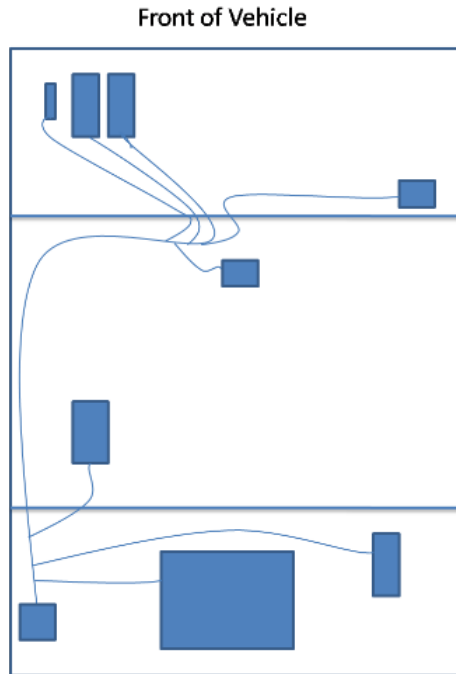


Figure 76: Old ERAU CAN

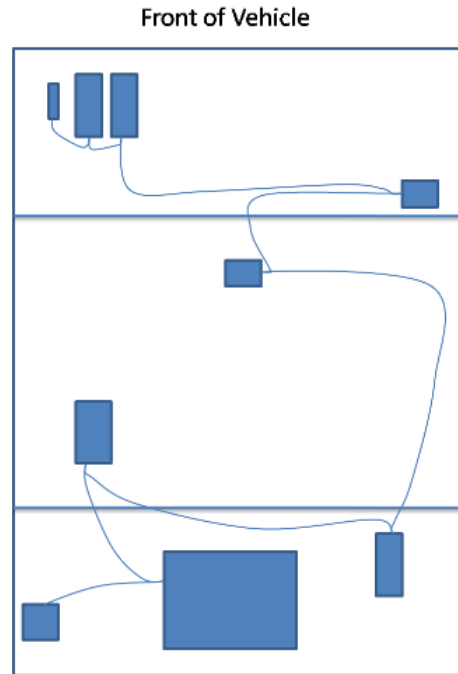


Figure 77: New ERAU CAN

In order to keep bus utilization low as new components were added to the vehicle it became necessary to install additional CAN networks in the vehicle. In addition to ERAU CAN, the SCR and Engine CAN networks are used. Figure 78 shows the signal layout for the vehicle.

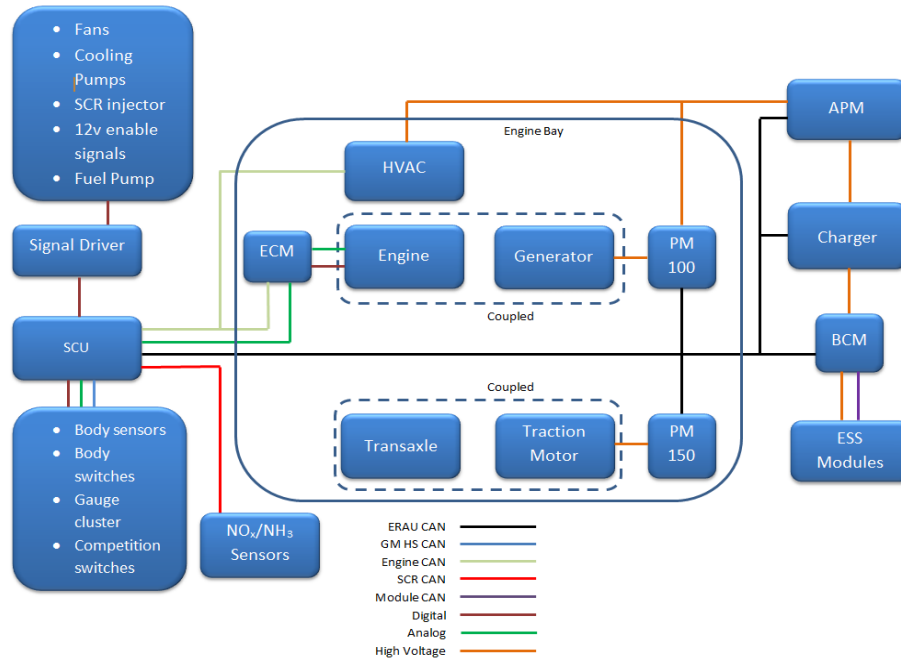


Figure 78: Vehicle signal Diagram

## 8.4 HV charging system design

Two different approaches were utilized for vehicle charging. The first was a passive approach using passive electrical components, two resistors and a diode, to initiate charging. This method proved to work for some EVSE chargers; however, it did not work for all chargers. The issue was due to not following the proper protocol for control pilot states. Table 7 shows the states used in the SAE J1772 protocol. The passive approach hardwires a diode and two resistor into the circuit, Figure 79, which makes the control pilot go directly to state C. This makes the EVSE supply power to the vehicle immediately when plugged in. This method can and will work for some EVSEs; however, if states are skipped some EVSEs will signal an error has occurred and will not provide power to the vehicle. To make all EVSEs compatible with the vehicle the states have to follow the proper order

starting with state A, then B, and finally C. The passive approach skips state B while going straight to C. To fix this issue, an active approach is used in place of the passive.

Table 7: Control Pilot and Proximity States [15]

State	Pilot High (V)	Pilot Low (V)	Frequency (Hz)	Proximity (V)	Description
A	+12	N/A	DC	4.5	Not Connected
B	+9	-12	1000	3.0	EV Connected
C	+6	-12	1000	1.5	EV Charge

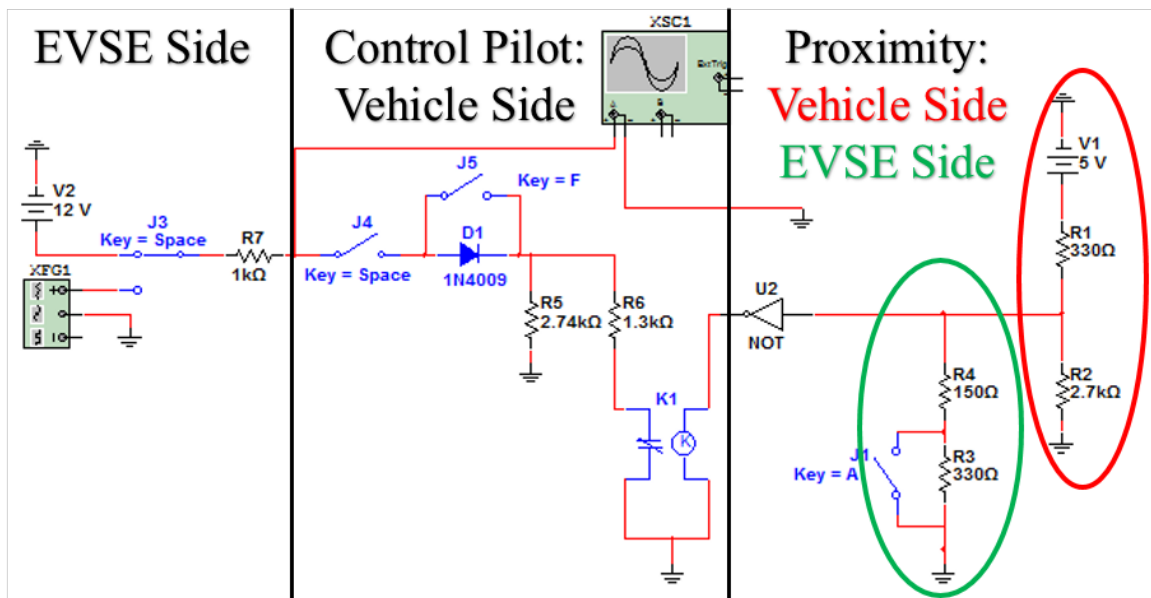


Figure 79: Charging Simulation

The second approach switches a resistor, R6, to ground, and can be seen in Figure 79. The passive approach has Resistor R6 connected to ground at all times. The vehicle is

able to change between state B and C by being able to actively connect and disconnect resistor R6 to ground. When R6 is disconnected from ground control pilot will be able to enter state B, and when R6 is connected to ground state C will be entered. To accomplish this a microcontroller, Figure 80, is used to actively monitor and control the charging initiation process.

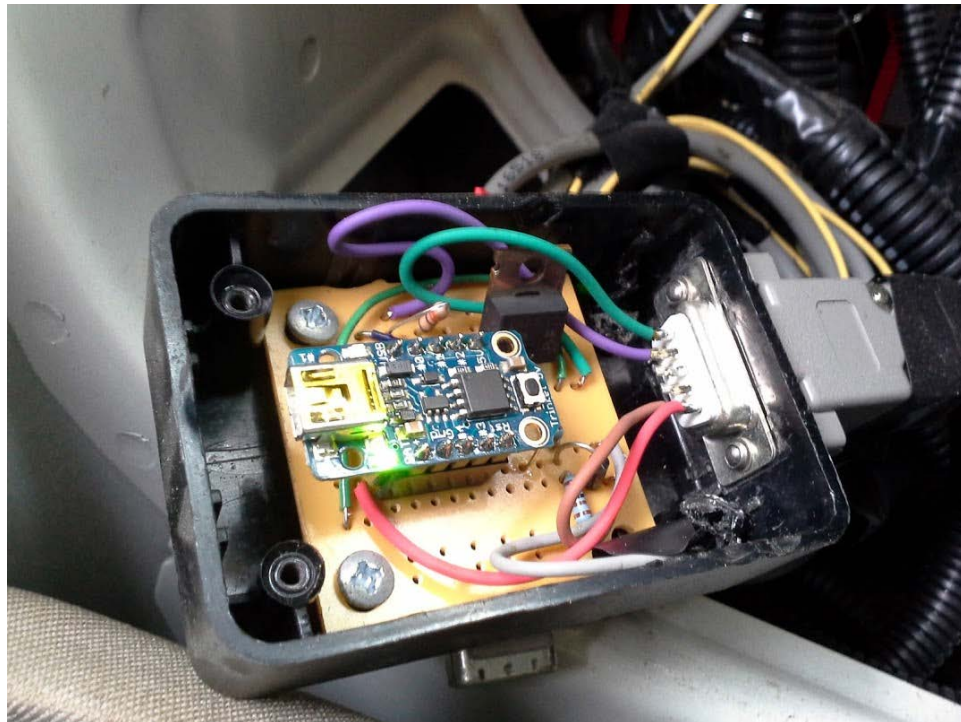


Figure 80: Vehicle Proximity and Control Pilot Controller

A Trinket mini microcontroller, made by Adafruit, was purchased, and programmed to properly handle charging initiation for the vehicle. With this controller any level 1 or level 2 charger using the SAE J1772 standard can be used to charge the vehicle. This controller was chosen for its small size of 1.2" x 0.6", and low power draw of 9mA. Its main function is to monitor the proximity signal voltage and switch resistor R6 to ground when appropriate. Table 7 gives the proximity voltage seen in each control pilot state.

The program written for the Trinket is given below.

```
int PROX = 1;
int charge = 1;
int val = 0;

void setup () {
    pinMode(charge, OUTPUT);
    digitalWrite(charge, LOW);
}

void loop () {
    val = analogRead(PROX);
    if (val < 368 && val > 246 ) {
        delay(5000);
        digitalWrite(charge, HIGH);
    }

    else {
        digitalWrite(charge, LOW);
    }

    delay(250);
}
```

The code works as follows. Analog pin 1, PROX, is used to read proximity voltage, and digital pin 1, charge, is set to an output. Charge is connected to the gate pin of an n-channel mosfet. When charge is LOW the mosfet is off which disconnects resistor R6 from ground, and keeps control pilot in state B. When charge is HIGH, the mosfet connects resistor R6 to ground, and control pilot enters state C. The main loop reads the proximity voltage to check that it is within range for state C. State C voltage should be equal to 1.5V; however, to account for noise in the signal a range of 1.8V to 1.2V is used. This allows the signal to deviate by 0.3V higher or lower from 1.5V. If the signal is within the correct range charge goes high after five seconds to turn the mosfet on. PROX is continuously monitored to catch when the vehicle is unplugged, and this can be detected fast enough to turn the



mosfet off to return to state B before the plug is removed from the vehicle. This ensures the EVSE powers down to prevent arcing at the contacts for the charge port. This is important to ensure longevity of the contacts.

The diode in the control pilot circuit ensures an extra level of safety for charging. In state B and C the EVSE outputs a  $\pm 12\text{V}$  1 kHz square wave. The diode is located on the vehicle, so when the EVSE is connected to the vehicle the positive portion of the square wave is only affected by the control pilot circuitry. The negative portion cannot pass through the diode latching the voltage to stay at  $-12\text{V}$ . If the EVSE detects the negative side of the square wave is at  $-12\text{V}$  then the EVSE can provide power to the vehicle. The correct pilot sequence with a diode is seen in Figure 81.

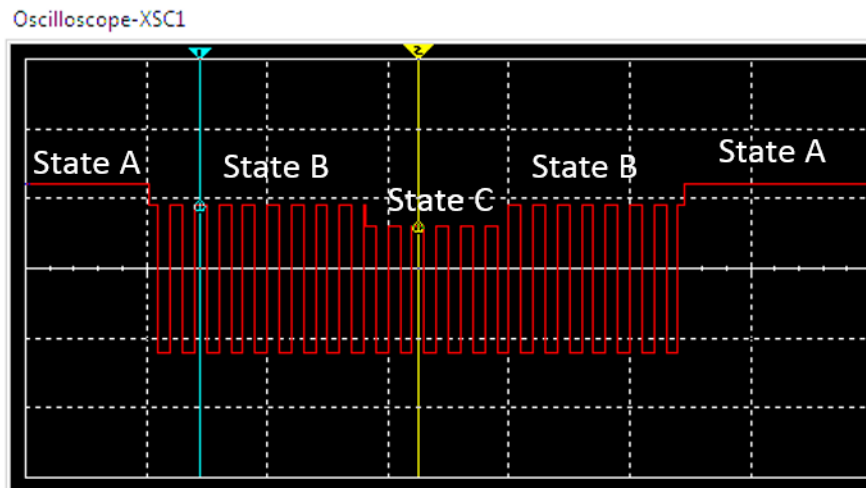


Figure 81: Control Pilot Normal Operation

If the EVSE ever sees the negative half of the square wave change from  $-12\text{V}$  it will not provide power. This prevents accidental shock if the EVSE plug falls into a puddle or an object is stuck into the EVSE plug. Figure 82 shows what the EVSE will see if there

is no diode in the control pilot circuit. Both the positive and negative halves of the square wave are affected evenly. When this scenario is detected the EVSE will display a fault, and will not allow power to flow to the connector.

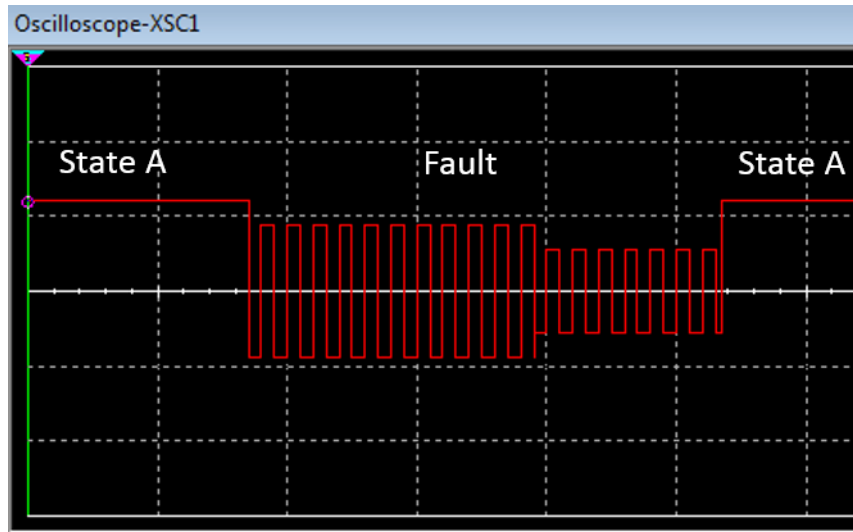


Figure 82: Control Pilot Fault

Figure 83 and Figure 84 shows data collected from the BRUSA charger during charging of the ESS. Level 1 and 2 EVSEs were used to show the power output for each mode.

	Limit:	Actual:
Batt Voltage [V] :	333.00	296.55
Total BattCurr[A]:	8.10	3.15
Charger Batt Current [A] :		3.15
Bypass Batt Current [A] :		NONE
Charging Profile Section #:		1
Charging Profile Phase :		I
Charger Mains Voltage [V] :		114.60
Chg Mains Pwr [W]:	3680.00	1031.40
Chg Mains Curr[A]:	50.00	9.00
Total Mains Current [A] :		9.00

Figure 83: Level 1 120V Charge

	Limit:	Actual:
Batt Voltage [V] :	333.00	298.60
Total BattCurr[A]:	16.20	11.20
Charger Batt Current [A] :		11.20
Bypass Batt Current [A] :		NONE
Charging Profile Section #:		1
Charging Profile Phase :		I
Charger Mains Voltage [V] :		237.60
Chg Mains Pwr [W]:	3680.00	3694.68
Chg Mains Curr[A]:	50.00	15.55
Total Mains Current [A] :		15.55

Figure 84: Level 2 220V Charge

## 8.5 Vehicle Testing

### 8.5.1 GM vs. ERAU Drive Test Results

Table 8 provides the general data post processed from the vehicle logs. It is important to note that regenerative braking was disabled during the GM test and enabled for the ERAU test. Based on this fact, it can be clearly seen that regenerative braking had a major impact on the performance of the vehicle. The Charge Deplete distance gained 12.45 miles before the diesel generator had to turn on to supply power to the vehicle. Also, the overall power used per mile was reduced from 498 to 340 Wh/mi.

Table 8: Vehicle Test Data

	GM Test	ERAU Test
Charge Deplete Distance	26 mi	38 mi
Charge Sustain Distance	72.9 mi	23.3 mi
kWh/mile	0.498	0.340
Fuel consumed	3.2 gal	0.7 gal
Diesel MPG	23	35
Distance Traveled	98.9 mi	61.8 mi
Max Range	171.78 mi	264.59 mi

By recovering energy with regenerative braking, vehicle efficiencies were increased. This allowed the diesel generator to operate in a reduced power mode as seen in Figure 85 and Figure 86.

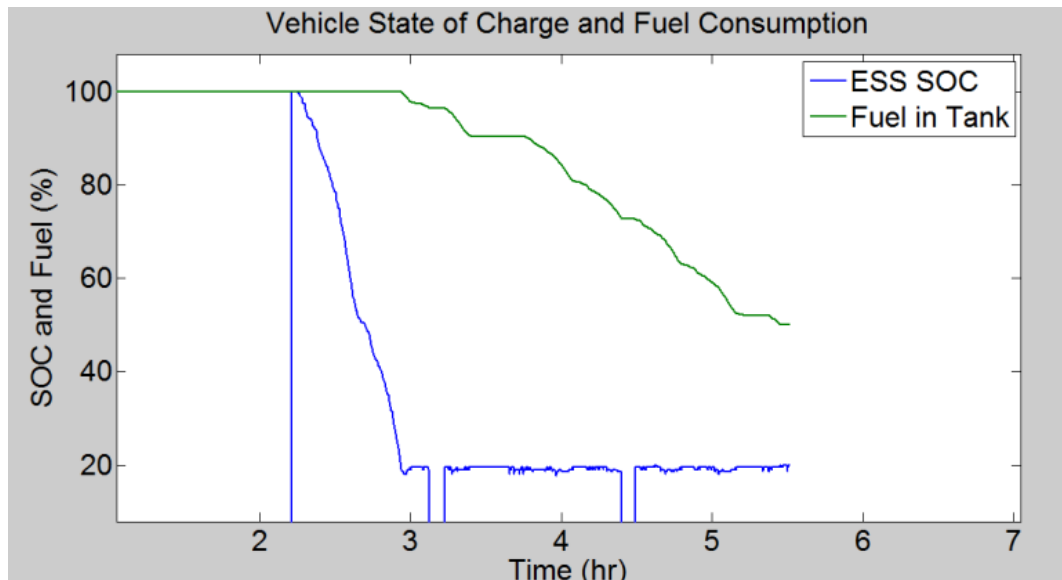


Figure 85: GM Test Data

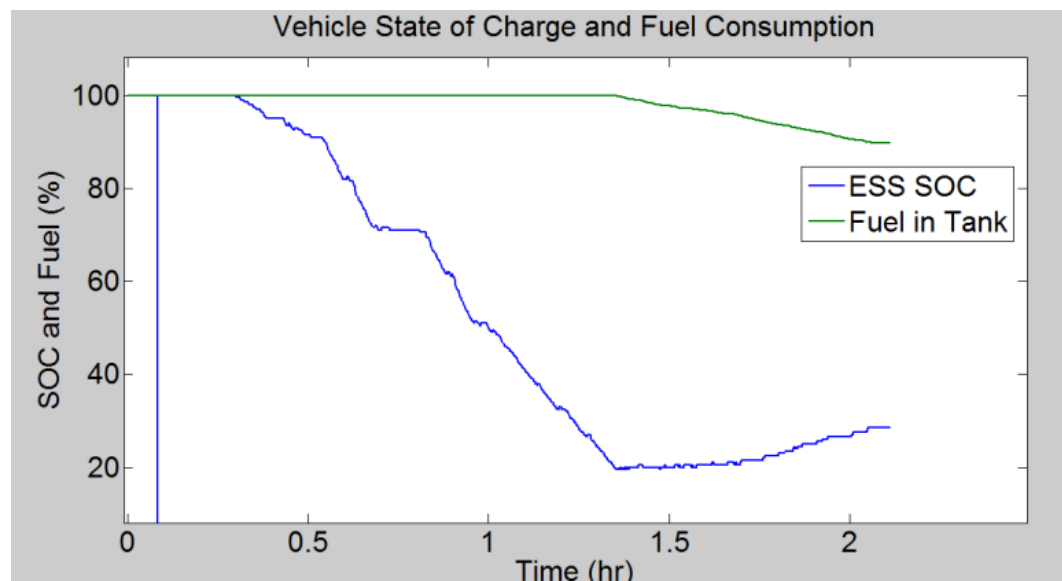


Figure 86: ERAU Test Data

Figure 85 shows that once the ESS dropped to a SOC of 20% the Diesel turned on and began generating power to sustain driving. The SOC stayed very close to 20% for the

duration of the drive schedule; however, Figure 86 reveals the duration of time increased by more than 20 minutes before the diesel engine turned on. Once the diesel engine turned on the SOC was maintained at 20% SOC with sustained highway driving.

Once the vehicle returned to city driving conditions the SOC began to rise. This was caused by the increased braking inherent to city driving; thus, regenerative braking supplied enough power to the ESS to raise the level of the SOC. Testing concluded with a SOC of 30%. At 35% SOC the diesel engine would have shutdown to allow the vehicle to solely run off the ESS, but the diesel generator also reduced the amount of power being generated since the regenerative braking was able to supplement the generator. This allowed fuel to be consumed at a slower rate and increase the efficiency of the diesel generator.

### 8.5.2 Zero to Sixty

Figure 87 gives testing data performed for a 0 to 60 test. It is important to note that the current in the graph was divided by 10. The data shows that the vehicle was able to do 0 to 60 in 9.56s. Once 60 miles per hour was reached the driver released the accelerator pedal which engaged the regenerative braking. At 19 seconds the regenerative braking generated about 250A back into the ESS.

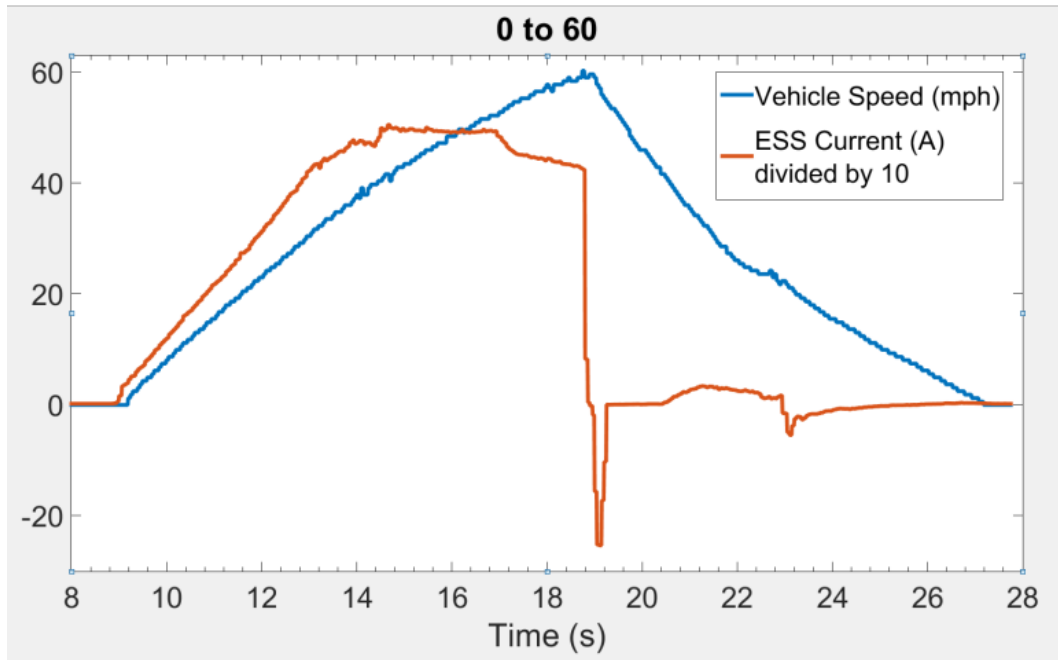


Figure 87: Vehicle 0 to 60 mph data

During testing, it was noted that the voltage of the high voltage system would sag. This caused the power delivered to the traction motor to decrease. To alleviate the voltage sag the diesel generator was turned on before the 0 to 60 run was performed. The generator ran at maximum performance, and kept at maximum performance for the duration of the 0 to 60 test. This enabled the vehicle to reduce its 0 to 60 time by 0.5 seconds. This gave a new 0 to 60 time of about 9.0 seconds.

### 8.5.3 Regenerative Braking

Data collected During the ERAU drive test is given in Figure 88. This portion of data specifically demonstrates the regenerative braking controls operating on the vehicle while exiting the highway, I-95, on an off ramp, and stopping the vehicle at a traffic light. While the acceleration pedal is kept steady to maintain vehicle speed of about 70 mph the

ESS current is relatively steady. As the driver lifts their foot from the accelerator pedal the regenerative braking will engage, and the rate of the accelerator being depressed governs how aggressive the regenerative braking will be.

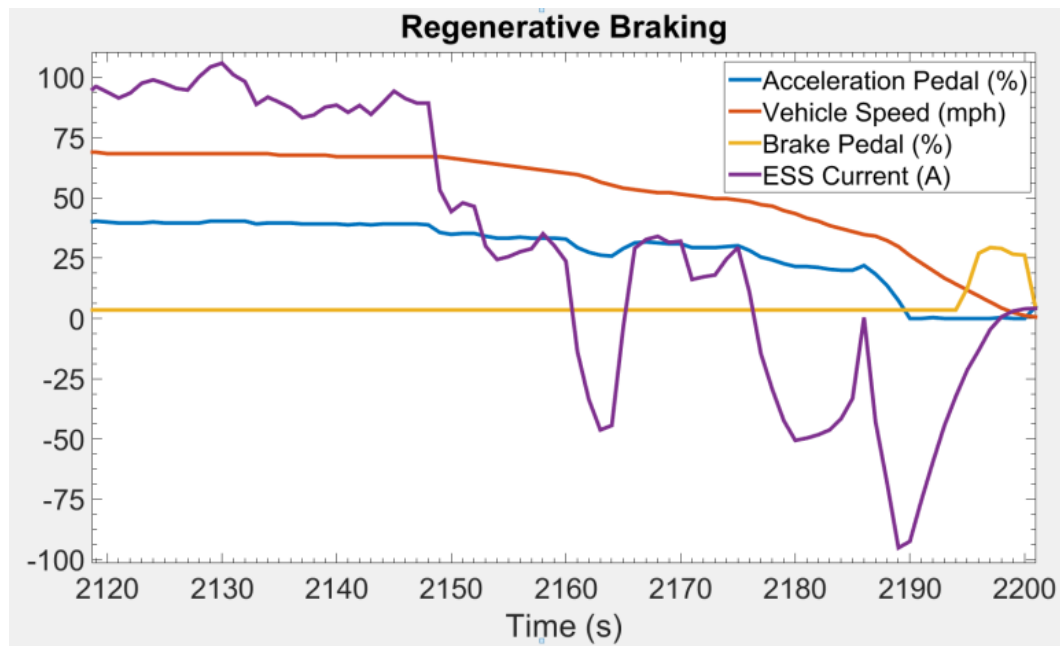


Figure 88: Regenerative Braking Data

At 2150 s the driver begins to lift off of the accelerator pedal. This slows down the vehicle as it exits the highway. Initially, the vehicle slows as expected and slows down gradually. At the times of 2160 s, 2175 s, and 2185 s the driver lifts off the accelerator pedal more sharply. At these times regenerative braking engaged. This generated a current that went back into the ESS, and can be seen due to the current changing from positive to negative.

Up until 2185 s and these three regenerative braking events the vehicle the vehicle's speed has changed from 70 mph to 14 mph in 45 s without pressing the brakes. On average, the vehicle decelerated at a rate of 1.24 mph/s; however, during regenerative braking the vehicle decelerated at a greater rate. This is especially seen at the time of 2185 s. At this point, the driver lifts off the accelerator pedal completely, 0% accelerator pedal pressed, from about 25%. This commands the greatest regenerative event represented on the above plot, and causes the vehicle to decelerate at 2.18 mph/s. At 14 mph the driver finally presses the brake to stop at the traffic light. This improves consumer acceptability by enabling the driver to essentially control the vehicle's acceleration and deceleration with the accelerator pedal. This makes it so brakes are used for the final stopping of the vehicle, or for when extra braking is needed for safety. Since the brakes do not to be used as much, the life of the brakes will be extended.

#### 8.5.4 Side Skirts Aero Test

Figure 89 and Figure 90 shows the data collected during a aerodynamic test performed on Interstate 95 near Daytona Beach. The test was performed on a 3.2 mile stretch of the interstate, and two separate tests were performed. Each test consisted of driving the vehicle north bound on I-95, the vehicle gets off the highway, and then drives south bound to return to the starting location. Speed was maintained at 70 mph as much as possible, but was reduced if needed depending on traffic conditions to maintain safety. Test one was performed without side skirts installed on the vehicle, and test 2 was performed with the side skirts installed.



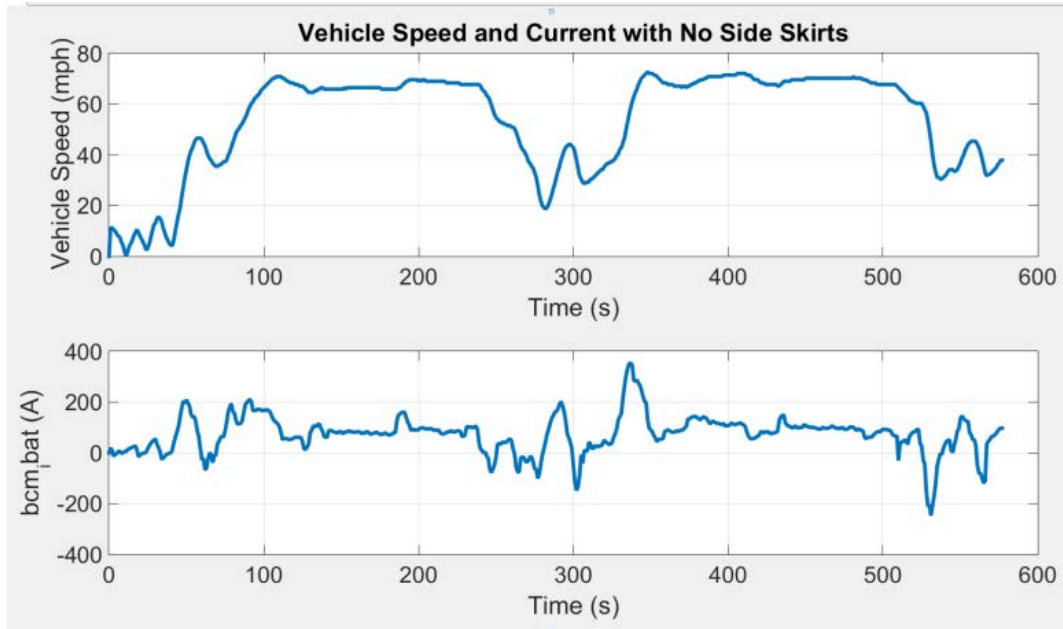


Figure 89: Aero Test No Side Skirts

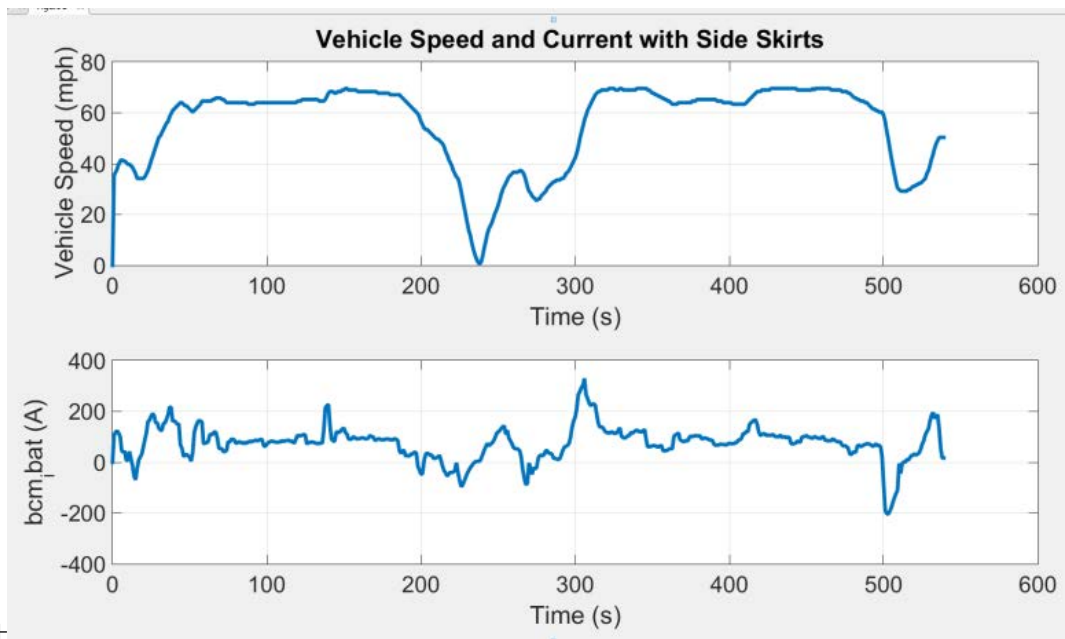


Figure 90: Aero Test with Side Skirts

By averaging the currents from each test, it was found that having the side skirts installed on the vehicle generated more drag. This extra drag resulted in a 2 A increase of current with the side skirts on compared to having the skirts off. Due to the extra current

needed being fairly small, the range of the vehicle was not impacted. More testing will be performed to validate the viability of the side skirts.

## 8.6 HV Distribution Box Design

To aid the team in component calibration and testing for EcoCAR 3. A HV demo box has been designed specifically for bench testing of HV components within the lab. The demo box will also serve as a tool to teach students HV safety and good practices. Figure 91 through Figure 98 shows how to properly prepare the HV cable with shielding. In order to avoid a short between the main copper conductor and the shielding it is important to take proper measurements for proper separation. Rule of thumb for arc distance of a given voltage is 3 MV/m. Using this rule, 3 kV needs at most a 1 mm air gap to be able to jump.



Figure 91: HV Cable step 1



Figure 92: HV Cable step 2



Figure 93: HV Cable step 3



Figure 94: HV Cable step 4



Figure 95: HV Cable step 5



Figure 96: HV Cable step 6



Figure 97: HV Cable step 7



Figure 98: Cable Ends

Heat shrink is used on the HV cables to secure the shielding and insulation. If heat shrink is not used the insulation will pull back on the cable exposing the shielding underneath. The shielding will also fray if the ends are not secured with heat shrink.

Figure 99 through Figure 106 depicts the main components for the HV distribution box. The main body is an electrically rated plastic enclosure with a mounting plate. The plate is used to secure the hardware installed in the box, and the plate will also act as a grounding plate. Copper shielding is utilized with the cable glands to allow continuity between all of the HV cables attached to the box. Plexiglas is used in order to add safety and separation between HV and GND. Fiberglass standoffs, made by Glastic, are also used to insulate the HV bus bars.

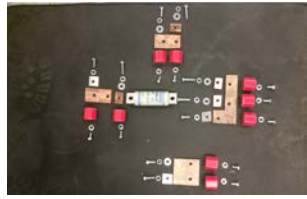


Figure 99: HV Hardware



Figure 100: Plexiglas



Figure 101: Separators



Figure 102: Copper

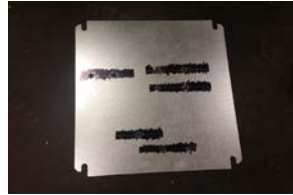


Figure 103: GND Plate



Figure 104: Enclosure

### Shielding



Figure 105: Gland Apart



Figure 106: Gland Together

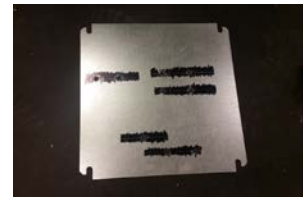


Figure 107 through Figure 115 details the actual build process. Holes are drilled through the box and copper mesh to allow the cable glands to be installed. First, the copper mesh is inserted into the box. The GND plate is then installed, followed by the Plexiglas mold. The standoffs are then bolted into place to hold everything together. The HV fuse and buss bars are installed and bolted into place. With the main hardware in place, the cable glands can now be installed. The HV cables are inserted through the glands and bolted to the buss bars. The shielding is left bare on small sections of the cables to allow the shield

to contact the cable gland insert. The HV test connector and HVIL micro switch are then installed. Finally, Kapton tape is used to add insulation to all conductors.

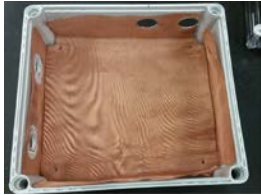


Figure 107: Shielding in Box

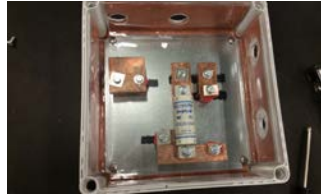


Figure 108: Plate with Hardware

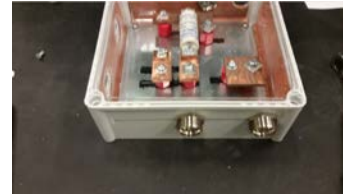


Figure 109: Glands Installed



Figure 110: Cables Installed



Figure 111: Test Conn. & HVIL



Figure 112: Box Insulated



Figure 113: Box Labels 1



Figure 114: Box Labels 2



Figure 115: Box Labels 3

The HV test connector, Figure 116, will allow for measurements to be taken, and will also be used to test for isolation and ground faults. To add an extra layer of safety, A HVIL micro switch is used to prevent the HV box from being energized.

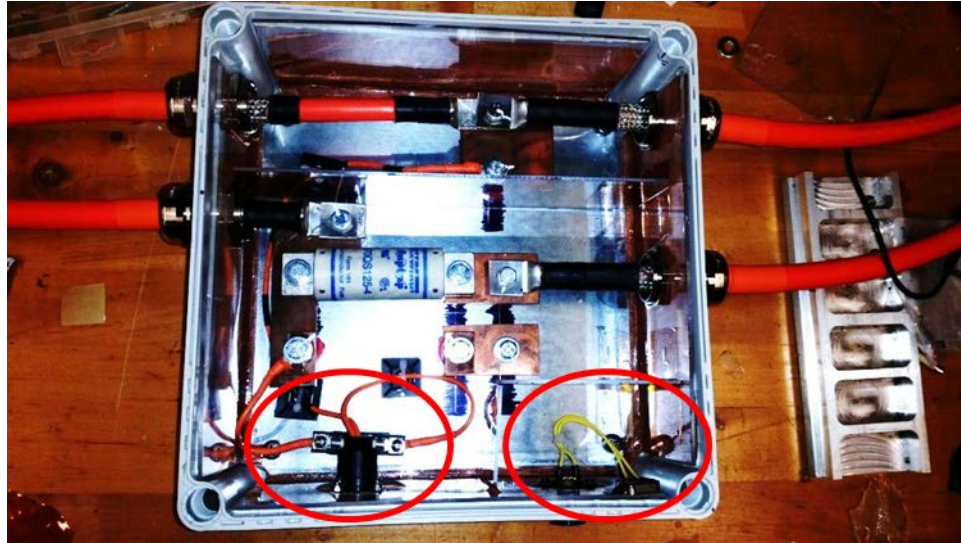


Figure 116: HV test Connector and HVIL Micro Switch

The completed HV distribution box can be seen in Figure 117.

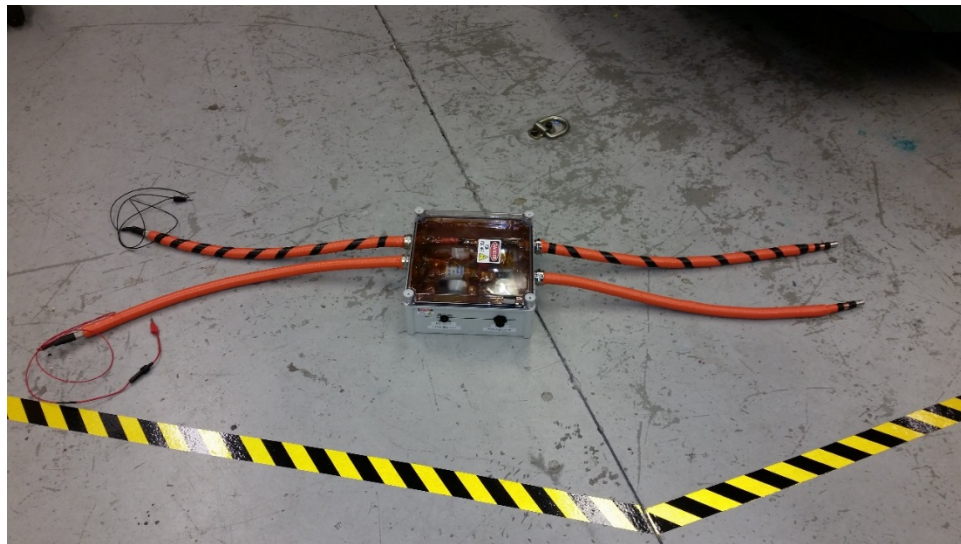


Figure 117: HV Box Complete

## 8.7 HV Simulation

Table 9 gives the values calculated with a Matlab script. Due to the size of this script it is not included within this paper. These calculated values are used in the Simulink model of the high voltage bus. By using these values the model is able to more precisely estimate the voltage ripple and resonant frequency. The resonant frequency is also calculated in the Matlab script. This value is more of an estimate for the system since it does not take in consideration the dynamics of the bus. This value is used to help zero in on the real resonant frequency by adjusting the output frequency of the pulse generators in the inverters. The goal of this simulation is to find these characteristics during a worst case scenario; therefore, the model tries to match what the high voltage bus will see during a 0 to 60 acceleration of the vehicle. This is where the most stress is exerted on the high voltage bus.

Table 9: Simulation Calculated Characteristics

Total Wire Capacitance	0.37 nF
Total Load Capacitance	953.01 uF
Total System Capacitance	953.01 uF
Total System Inductance	0.13 uH
Res Frequency of ESS branch	4964.14 Hz
Res Frequency of BRUSA branch	119.47 Hz
Res Frequency of IMG Generator branch	7.27 Hz
Res Frequency of IMG Motor branch	7.27 Hz
Res Frequency of HVAC branch	29.28 Hz
HVAC Inductance	1.18 uH
Inverter Inductance	1.04 uH
ESS Inductance	6.89 uH
BRUSA Inductance	0.22 uH
Res Frequency of system	138.64 Hz

Figure 118, Figure 119, and Figure 120 shows the results when running the simulation with the inverter pulse generator commanded at 12 kHz. At this frequency the voltage ripple of the bus is seen to be 8 V peak to peak. Most high voltage components can handle a voltage ripple of 25 V peak to peak; therefore, 8V is well within acceptable bounds for the bus. The power spectral density block, Figure 118, also shows the frequencies seen on the bus. This reading is in radians/second. When converted, divide rad/sec by  $2\pi$ , the frequency is found to be 12 kHz. This is the same frequency as the output of the pulse generator, so this 12 kHz is not the resonant frequency. To find the resonant frequency the frequency needs to be changed in the pulse generator, and the spectral analyzer, Figure 120, and PSD block, Figure 118, are observed. As the frequency on the bus approaches the resonant frequency the power of the signal at the output frequency and the amplitude of the voltage ripple will increase. When the signal power and voltage amplitude reach a maximum the resonant frequency can be found.

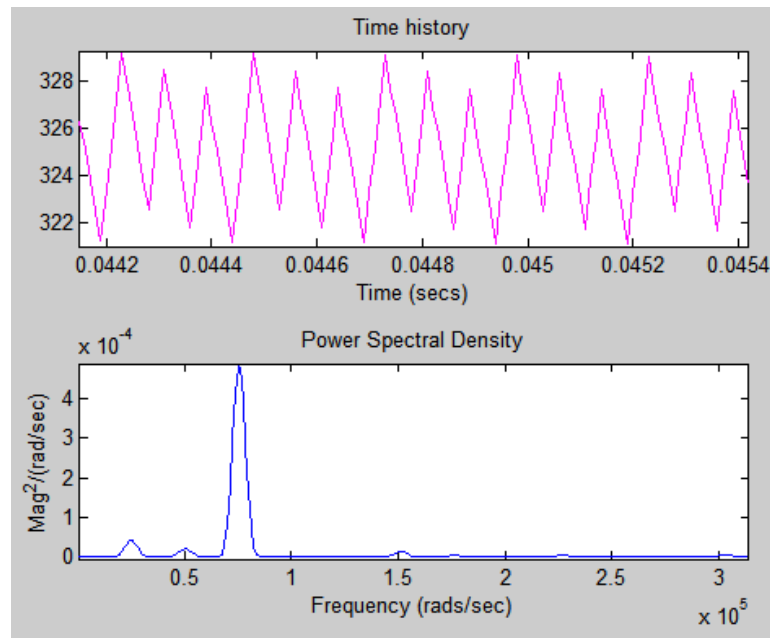


Figure 118: Power Spectral Density 12 kHz



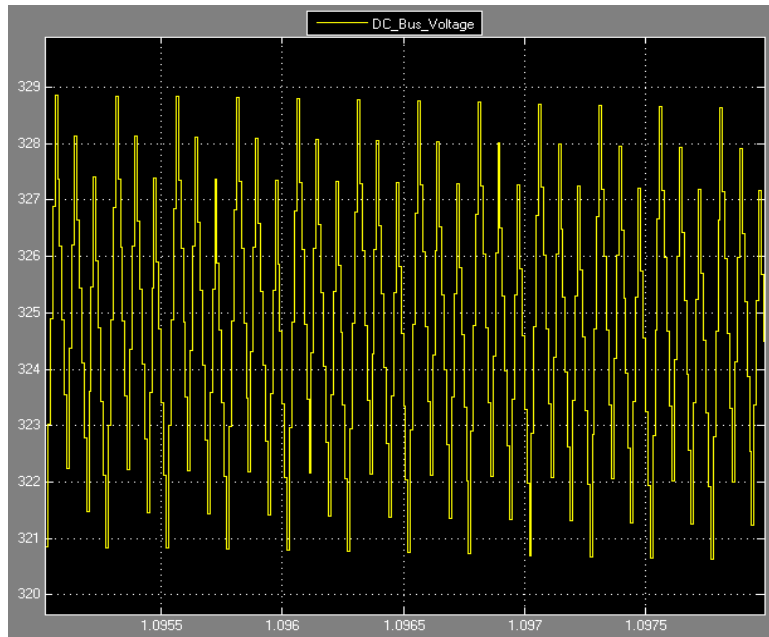


Figure 119: DC Bus Voltage 12 kHz

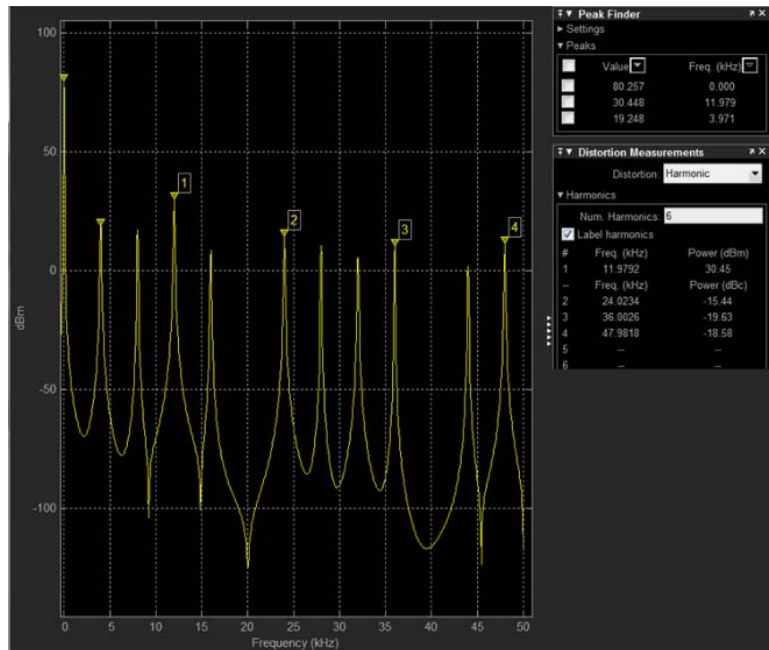


Figure 120: Spectrum Analyzer 12 kHz

The Simulation is not able to perform a frequency sweep across a range of frequencies. This is caused by the nature of the PSD and spectrum analyzer blocks. Due to this, the simulation has to be run for each frequency of interest. The simulation began at 12 kHz, and then a broad range of frequencies are chosen above and below 12 kHz. As the frequency decreased from 12 kHz the power a voltage ripple increased, while the power and voltage ripple decreased with frequencies above 12 kHz. This shows that the resonant frequency is below 12 kHz. The frequency was then decreased by 1000 until a peak was seen and then the signal power fell. This occurred at 1000 Hz. The frequency was then slowly decreased until the absolute peak was seen. Figure 121, Figure 122, and Figure 123 shows the data taken at the true resonant frequency of the high voltage bus at 911 Hz. At 911 Hz the signal power is at 54 dBm versus 30 dBm at 12 kHz, and the voltage ripple at 911 Hz is 60 V peak to peak versus 8 V peak to peak. At 60 V peak to peak, there is a definite certainty of component damage occurring. Specifically, the bulk capacitors will be damaged preventing the voltage from being properly smoothed.

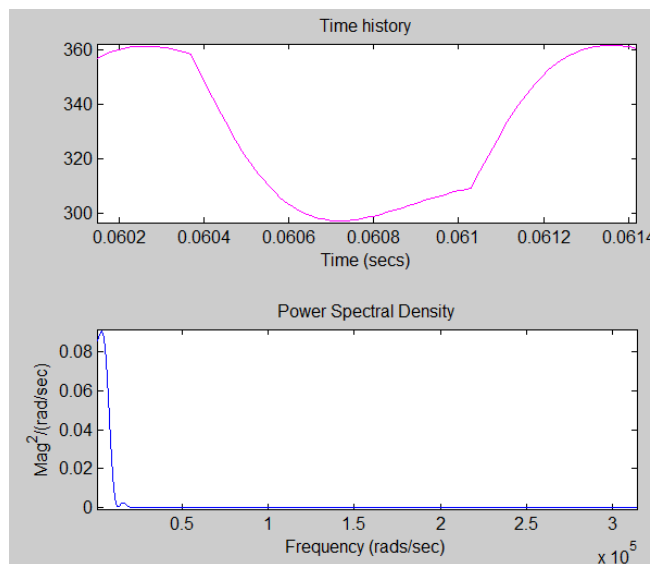


Figure 121: Power Spectral Density 911 Hz

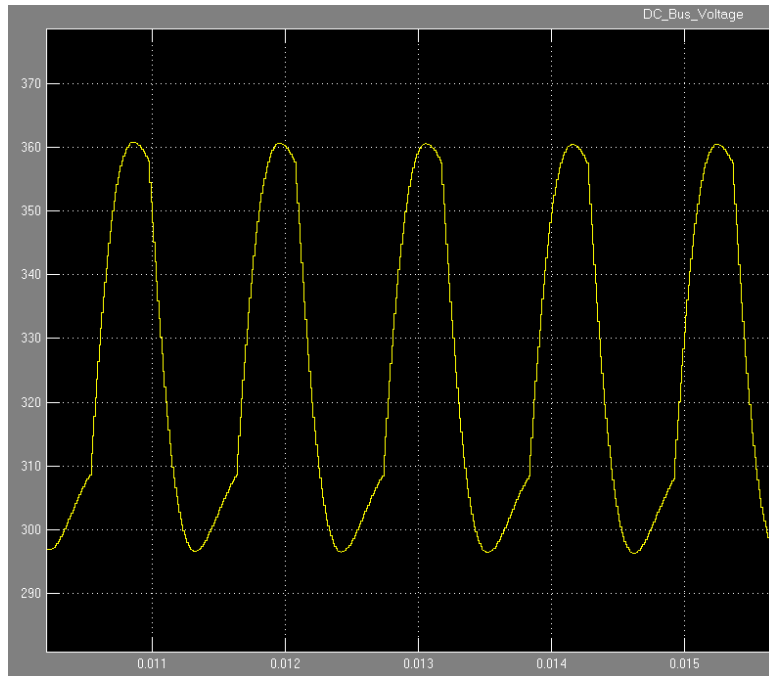


Figure 122: DC Bus Voltage 911 Hz

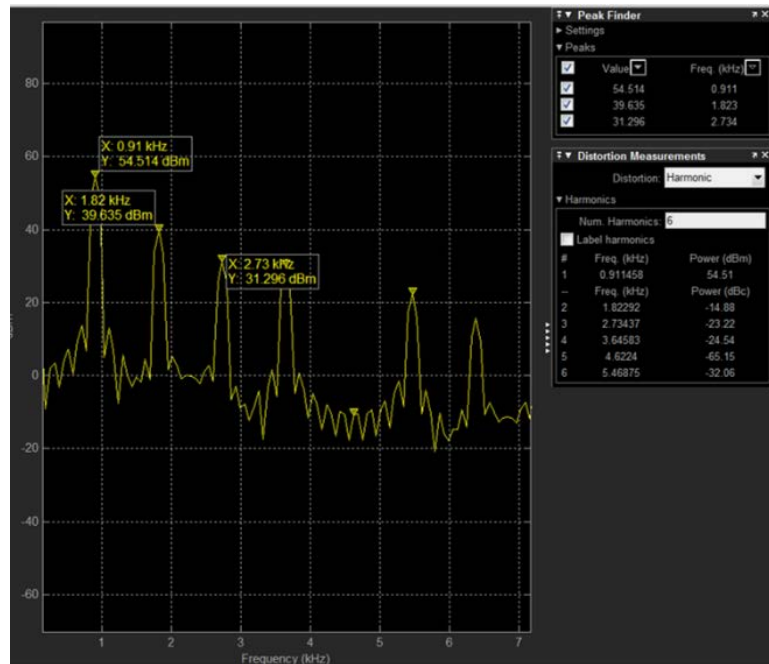


Figure 123: spectrum Analyzer for 911 Hz

Since inverters for electric vehicles typically switch at higher frequencies between 1 and 12 kHz the 911 Hz resonant frequency should not be a problem to avoid. Even better,

in dealing with inverters for EcoCAR 2, 12 kHz is where manufactures seem to shoot for with their inverters. It is currently not known what exact frequency is being used for the Bosch IMG inverters being used on the ERAU EcoCAR 3 vehicle; however, due to the resonant frequency being relatively low it should not cause an issues, or need any major modifications.

## **9. Conclusion**

At the end of EcoCAR 2 Y2 the vehicle was electrically in very bad shape. The HV systems were in the vehicle, and for the most part in good working order. The low voltage systems were not in good shape. The vehicle could not spin the wheels, the engine was never wired, an SCR system was not even designed, the ESS was not capable of being charged, and there were numerous wiring mistakes throughout the vehicle. There was an enormous amount of work to be done in order to get a properly functioning vehicle, but with the help of the ERAU team we were able to get a running vehicle. The team started at 13<sup>th</sup> place out of 15, and at the end of EcoCAR 2 Y3 we had taken 4<sup>th</sup> place. The quality of the teams work truly showed. Not only were we able to complete the needed electrical system implementation, but data was also able to be taken that was used to make systems run more efficiently. This was a feat that had never previously been accomplished. For EcoCAR 3 a high voltage distribution box and high voltage simulation were designed and built. The HV distribution box will be beneficial in bench testing HV components off the vehicle. This will allow the team to test and characterize HV components before they are installed in the vehicle. This will both save time and valuable resources. The HV simulation

will allow the team to better understand the HV system in the vehicle as a whole. Instead of hoping the system will work the team will be able to have confidence in their design by using the simulation to understand how the high voltage will react during vehicle operation. If a potential problem is observed, the team can take action and prevent a potential future issue.

## **10. Future work**

The EcoCAR 2 vehicle has been built and the team is moving all work to the EcoCAR 3 2016 Chevrolet Camaro. Because of this, the bulk of the future work should focus on improving the HV distribution box and HV simulation. The HV distribution box should be used as a tool for teaching high voltage safety and best building practices. The box can also have added circuits installed to test multiple components at once, and have extra data collecting instrumentation added for testing purposes. The HV simulation will need to have the components better characterized as more data is received for all the components. This will be especially true for the Bosch IMG inverters the team will be using. The inverters will cause the most stress on the high voltage bus; therefore, it is very important that the team understands the inverters. The more information added to the model will give the team the added benefit of understanding any potential issues during vehicle operation. The vehicle wiring portion of this thesis should be used as a guide for proper wiring and system design. Students new to the electrical team specifically will benefit from this thesis for proper wiring techniques. Vehicle instrumentation should be added into the EcoCAR 3 vehicle wiring. There was little time to implement this into the EcoCAR 2

vehicle, but it would have greatly improved data collection and troubleshooting on the vehicle. Extra sensors for taking voltage, current, and temperature measurements will be especially beneficial for vehicle testing and optimization of systems. This can be implemented on both the low voltage and high voltage vehicle systems; although, great care towards safety in the high voltage sensor instrumentation will need to be taken. Break out boxes could also be designed to plug in-line between a wiring harness and component for taking data and testing.

## 11. Bibliography

- [1] EcoCAR 2, "About EcoCAR 2 | EcoCAR 2: Plugging In to the Future," EcoCAR 2, 2011. [Online]. Available: <http://www.ecocar2.org/about-ecocar2>.
- [2] C. Rowe, I. Demirkiran, D. Bonderczuk and P. Currier, "An Approach to Enhance the Efficiency and Consumer Acceptability of a Series Plug-in Hybrid Vehicle," *SoutheastCon 2015*, pp. 1-7, 2015.
- [3] "Chaohui Liu; Jiabin Wang; Colombage, K.; Gould, C.; Sen, B.; Stone, D., "Current ripple reduction in 4kW LLC resonant converter based battery charger for electric vehicles," in Energy Conversion Congress and Exposition (ECCE), 2015 IEEE , vol., no., pp.60".
- [4] W. Liu, Introduction to Hybrid Vehicle System Modeling and Control, New Jersey: Wiley, 2013.
- [5] R. Dorf, The Electrical Engineering Handbook, CRC PRESS, 1993.
- [6] "Karvonen, Andreas; Thiringer, Torbjorn, "Co-Simulation and Harmonic Analysis of a Hybrid Vehicle Traction System," in Vehicle Power and Propulsion Conference (VPPC), 2015 IEEE , vol., no., pp.1-6, 19-22 Oct. 2015".
- [7] "Okura, K., "Development and Future Issues of High Voltage Systems for FCV," in Proceedings of the IEEE , vol.95, no.4, pp.790-795, April 2007".

- [8] "Anwar, M.N.; Gleason, S.E.; Grewe, T.M., "Design considerations for high-voltage DC bus architecture and wire mechanization for hybrid and electric vehicle applications," in Energy Conversion Congress and Exposition (ECCE), 2010 IEEE , vol., no., pp.877-8".
- [9] N. T. STANDARD, "CRIMPING, INTERCONNECTING CABLES, HARNESSSES, AND WIRING," National Aeronautics and Space Administration, 2011.
- [10] "GM Upfitter Integration: Electrical Best Practices," 2015. [Online]. Available:  
[https://www.gmupfitter.com/files/media/photo/623/New\\_Elect\\_BP\\_05\\_27\\_15.pdf](https://www.gmupfitter.com/files/media/photo/623/New_Elect_BP_05_27_15.pdf). [Accessed 2015].
- [11] National Aeronautics and Space Administrator, "NASA Workmanship Standards," [Online]. Available:  
<http://workmanship.nasa.gov/lib/insp/2%20books/frameset.html>. [Accessed 2015].
- [12] T. V. Johnson, "Diesel Emissions in Review," *SAE International Journal of Engines*, vol. 4, no. 1, pp. 143-157, 2011.
- [13] T. V. Johnson, "Vehicular Emissions in Review," *SAE International Journal of Engines*, vol. 7, no. 3, pp. 1207 - 1227, 2014.
- [14] BOSCH, Automotive Handbook, Robert Bosch GmbH, 2011.
- [15] "SAE J1772," Wikimedia Foundation, 1 November 2015. [Online]. Available: [https://en.wikipedia.org/wiki/SAE\\_J1772](https://en.wikipedia.org/wiki/SAE_J1772).



- [16] D. Barsotti and S. Boetcher, "OPTIMIZING JETS FOR ACTIVE WAKE CONTROL OF GROUND VEHICLES," *Proceedings of the ASME 2013 International Mechanical Engineering Congress & Exposition IMECE 2013. San Diego..*
- [17] C. P. Rowe II, D. Bonderczuk, C. M. Rowe, Y. Meng and P. N. Currier, "Refinement and Optimization of a Series Plug-In Hybrid Electric Vehicle with a B20 Bio-Diesel Generator as Part of EcoCAR 2: Plugging into the future," 2014.
- [18] A. D'Hooge, R. Palin and S. Johnson, "The Aerodynamic Development of the Tesla Model S - Part 2: Wheel Design Optimization," 2012. SAE 2012 World Congress & Exhibition. Detroit..
- [19] H. Khalifi, "Hybrid electric power system validation through parameter optimization," Embry-Riddle Aeronautical University, Daytona Beach, 2015.